ACS SyntheticBiology

pubs.acs.org/synthbio

Research Article

The *Neurospora crassa* Inducible Q System Enables Simultaneous Optogenetic Amplification and Inversion in *Saccharomyces cerevisiae* for Bidirectional Control of Gene Expression

Makoto A. Lalwani, Evan M. Zhao, Scott A. Wegner, and José L. Avalos*

Cite This: https://doi.org/10.1021/acssynbio.1c00229

Read Online

ACCESS | Metrics & More | Article Recommendations | Supporting Information

ABSTRACT: Bidirectional optogenetic control of yeast gene expression has great potential for biotechnological applications. Our group has developed optogenetic inverter circuits that activate transcription using darkness, as well as amplifier circuits that reach high expression levels under limited light. However, because both types of circuits harness Gal4p and Gal80p from the galactose (GAL) regulon they cannot be used simultaneously. Here, we apply the Q System, a transcriptional activator/inhibitor system from *Neurospora crassa*, to build circuits in *Saccharomyces cerevisiae* that are inducible using quinic acid, darkness, or blue light. We develop light-repressed OptoQ-INVRT circuits that initiate darkness-triggered transcription within an hour of induction, as well as light-activated OptoQ-AMP circuits that achieve up to 39-fold induction. The Q System does not exhibit crosstalk with the GAL regulon, allowing coutilization of OptoQ-AMP circuits with previously developed OptoINVRT circuits. As a demonstration of practical applications in metabolic engineering, we show how simultaneous use of these circuits can be used to dynamically control both growth and production to improve acetoin production, as well as enable light-tunable co-production of geraniol and linalool, two terpenoids implicated in the hoppy flavor of beer. OptoQ-AMP and OptoQ-INVRT circuits enable simultaneous optogenetic signal amplification and inversion, providing powerful additions to the yeast optogenetic toolkit.

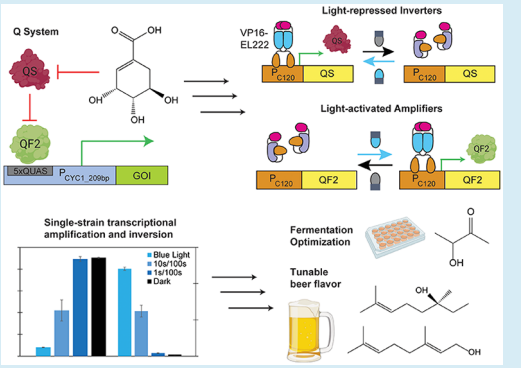

KEYWORDS: *inducible transcriptional control, Saccharomyces cerevisiae, optogenetics, chemical inducer, metabolic engineering, dynamic control, gene circuits*

INTRODUCTION

Optogenetics has proven to be a powerful tool for establishing dynamic control over biological processes.[1] Light is relatively inexpensive and can be applied or removed instantly, making its effects easily tunable and reversible without needing to manipulate media composition or other process conditions. Such advantages make light a noninvasive and orthogonal control agent for nonphotosynthetic microbes, such as the baker's yeast *Saccharomyces cerevisiae*. In recent years, a bevy of photosensitive systems have been established to implement light controls in this popular model organism.[2] Such tools respond to specific wavelengths of light to modulate gene expression or protein−protein interactions and have been applied to both basic research and biotechnological applications. However, these applications have typically been limited to unidirectional control based usually on the presence (or on occasion absence) of light. Bidirectional control using both light and darkness simultaneously to trigger different responses within a single cell thus presents a useful additional modality of dynamic control in yeast.

Our group has developed suites of optogenetic circuits that use the engineered blue light-triggered transcription factor, VP16-EL222.[3] We first developed OptoEXP, in which light-activated VP16-EL222 directly induces transcription of genes of interest from its cognate P_{C120} promoter in yeast;[4] however, this expression system is relatively weak and prone to being constrained due to light penetration limitations. We also developed optogenetic inverter circuits that induce genes of interest with darkness, called OptoINVRT, which use VP16-EL222 and P_{C120} to control the expression of the Gal80p repressor of Gal4p. With this architecture, genes of interest, including metabolic enzymes, placed downstream of the Gal4p-activated *GAL1* promoter, P_{GAL1}, are repressed in blue light and induced by darkness.[4] Using these circuits, we were able to bidirectionally toggle between blue light-driven cell growth (using OptoEXP) and darkness-induced chemical

Received: May 20, 2021

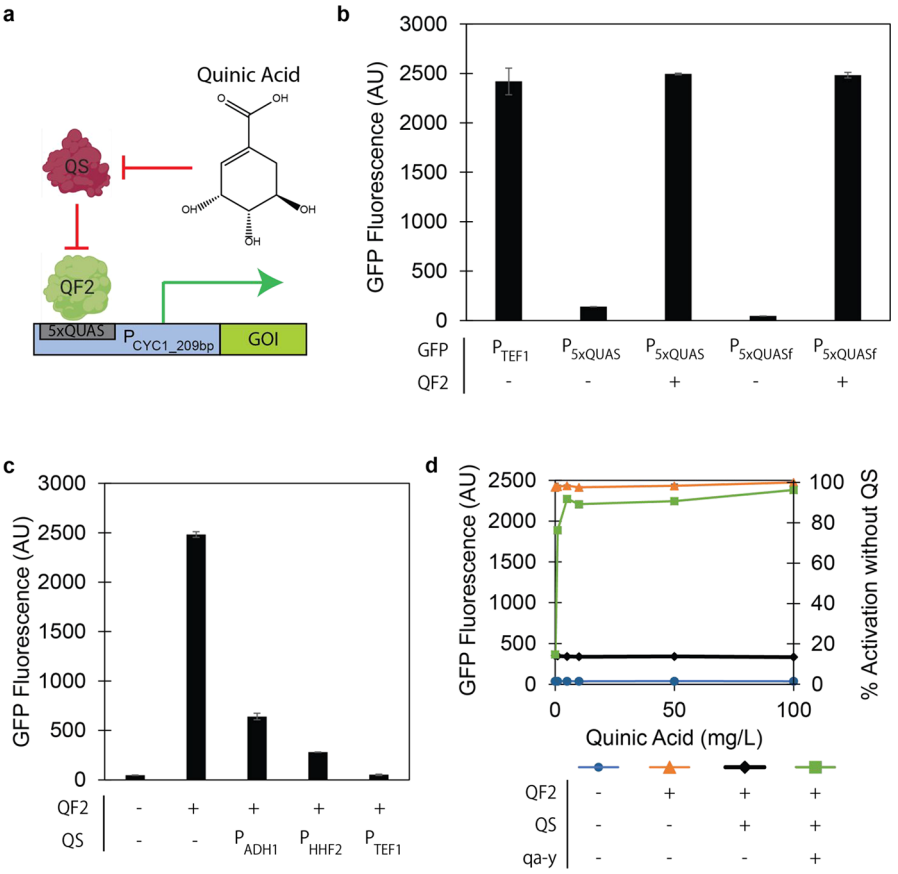

Figure 1. Q System functionality in *S. cerevisiae*. (a) QF2 binds to 5xQUAS operators embedded within a truncated P_{CYC1} promoter to activate transcription. QS inhibits QF2 activity, repressing transcription. QS repression of QF2 is inhibited by quinic acid. QF2 and QS proteins were created with Biorender.com. (b) GFP expression from P_{TEF1} (YEZ186), P_{5xQUAS} (yMAL49), P_{5xQUAS} with QF2 (yMAL53), $P_{5xQUASf}$ alone (yMAL49f), or $P_{5xQUASf}$ with QF2 (yMAL53f). (c) Repression of QF2-mediated GFP expression by QS transcribed from promoters of increasing strength: P_{ADH1} (yMAL110), P_{HHF2} (yMAL112), and P_{TEF1} (yMAL111). (d) GFP expression by QF2-activation of $P_{5xQUASf}$ without QS (yMAL53f, orange triangle); with QS (yMAL112, black diamond); or with QS and qa-y (yMAL321, green square), compared to a negative control (YEZ140, blue circle), in 0, 1, 5, 10, 50, or 100 mg/L quinic acid. All data shown as median values of 10 000 single-cell flow cytometry events; error bars (smaller than graphical icons in panel d) represent one standard deviation of replicates exposed to the same conditions (n = 3 biologically independent samples).

production (using OptoINVRT), including isobutanol fermentations in lab-scale bioreactors.[4] However, the weak transcriptional activity of P_{C120} in OptoEXP made it necessary to integrate multiple copies of the essential *PDC1* gene (to achieve blue light-dependent growth), leading to increased genetic burden. To overcome this limitation, we developed optogenetic amplifiers, or OptoAMP circuits, which increase the sensitivity and strength of the light-triggered transcriptional response. These circuits use VP16-EL222 (including a hypersensitive variant) to control expression of Gal4p, making promoters activated by this strong transcriptional activator, such as P_{GAL1}, P_{GAL10}, P_{GAL2}, and P_{GAL7}, become light inducible. The strength of these promoters, especially P_{GAL1} and its engineered derivatives, serve to further amplify the response of VP16-EL222 activation by ∼22 fold.[5] OptoINVRT and OptoAMP circuits thus enable strong and flexible gene expression under darkness and blue light, respectively, allowing for efficient light-controlled yeast fermentations in lab-scale bioreactors.[4,5]

While OptoINVRT and OptoAMP circuits individually provide dynamic control of yeast gene expression with light, they cannot simultaneously be used for bidirectional optogenetic control. Having the ability to strongly induce expression of different sets of genes with both light and dark conditions in the same strain would be an important advance. However, OptoINVRT and OptoAMP circuits cannot be simultaneously used in the same strain because they both harness the GAL regulon, using VP16-EL222 to control the expression of *GAL80* or *GAL4*, respectively. Therefore, to achieve simultaneous optogenetic amplification and inversion using our gene circuit architecture, it is necessary to develop new circuits that employ an orthogonal transcriptional regulon with minimal crosstalk with the GAL regulon.

The quinic acid (qa) gene cluster, or Q System, of the bread mold *Neurospora crassa* encodes a relatively simple regulon system for quinic acid metabolism,[6−8] which could be harnessed to develop new optogenetic circuits. It consists of a transcriptional activator QF, encoded by *qa-1f*, which binds to a specific 16-base pair upstream activating sequence (QUAS) in gene promoters. The Q System also contains a transcriptional repressor, called QS and encoded by *qa-1s*, which inhibits QF. The small molecule quinic acid inhibits QS to derepress QF, thereby allowing QF to transcribe genes involved in quinic acid catabolism.[9] The Q System has been successfully adapted for gene expression in various heterologous systems, including *Penicillium chrysogenum*,[10] fruit flies,[11]

https://doi.org/10.1021/acssynbio.1c00229
ACS Synth. Biol. XXXX, XXX, XXX−XXX

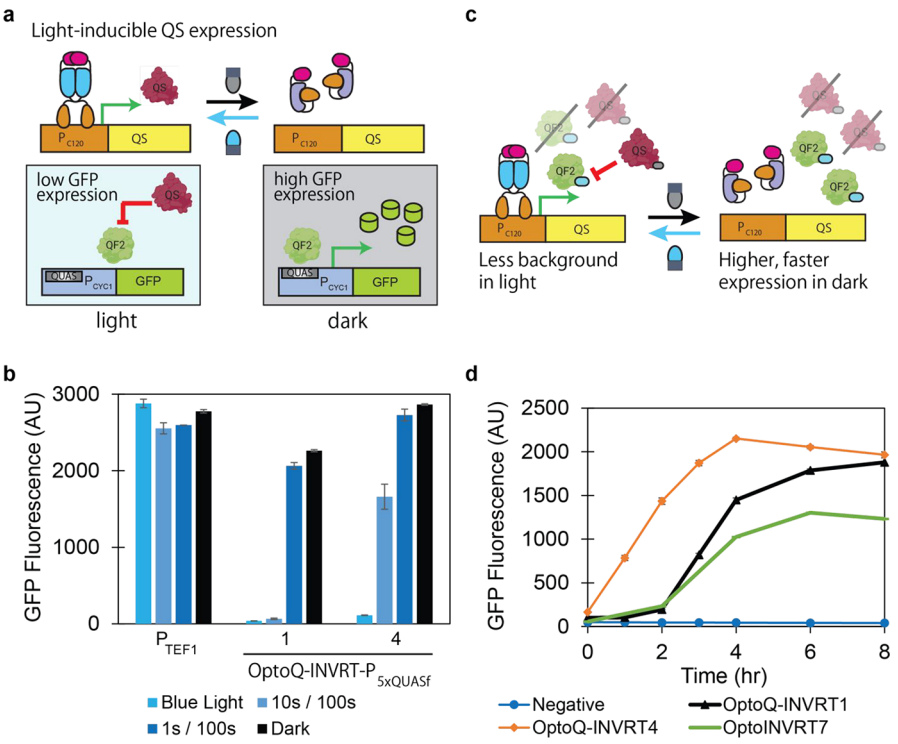

Figure 2. OptoQ-INVRT circuit characterization. (a) OptoQ-INVRT circuits invert the transcriptional signal of VP16-EL222 by transcribing QS from the P_{C120} promoter, which represses QF2 activity under blue light. Darkness prevents transcription of QS, which enables QF2-mediated transcriptional activation. (b) GFP expression from P_{TEF1} (YEZ186) or from $P_{5xQUASf}$ controlled by OptoQ-INVRT1 (yMAL227) or OptoQ-INVRT4 (yMAL239) under different doses of blue light: full light (100% light), 10 s ON/90 s OFF (10% light), 1 s ON/99 s OFF (1% light), and full darkness (0% light). (c) Tagging QS on the C terminus with the constitutive ODCmut degron (gray oval) increases expression levels in the dark and accelerates light-to-dark induction kinetics, while adding the photosensitive degron to the C terminus of QF2 attenuates (blue oval) increased leaky expression under blue light. (d) Time course of GFP expression from $P_{5xQUASf}$ controlled by OptoQ-INVRT1 (yMAL227, black triangle) and OptoQ-INVRT4 (yMAL239, orange diamond); and from P_{GAL1-M} controlled by OptoINVRT7 (YEZ230, green dash), compared to a negative control (YEZ140, blue circle). Strains were grown under blue light until exponential phase (OD_{600} = 0.8), then switched to darkness at t = 0. All data shown as median values of 10 000 single-cell flow cytometry events; error bars (smaller than graphical icons in panel d) represent one standard deviation of replicates exposed to the same conditions (n = 3 biologically independent samples). QF2 and QS proteins in (a) and (c) were created with Biorender.com.

HeLa cells,[11] nematodes,[12] zebrafish,[13] mosquitoes,[14] embryonic stem cells,[15] and plants,[16] but not *S. cerevisiae*. However, the portability of the Q System demonstrated in these studies suggested it might be functional in *S. cerevisiae* and possibly orthogonal to its GAL regulon, which would enable the development of new optogenetic circuits compatible with our existing OptoINVRT and OptoAMP circuits.

In this study, we show that the Q System is functional in *S. cerevisiae* and tractable to develop gene circuits in this yeast. QF can induce strong gene expression, which may be repressed by QS and induced with quinic acid. We use QF and QS to develop optogenetic inverter (OptoQ-INVRT) and amplifier (OptoQ-AMP) circuits that induce high levels of gene expression in darkness or blue light, respectively. Furthermore, the Q System does not exhibit crosstalk with the GAL regulon, allowing for the simultaneous use of optogenetic amplifier and inverter circuits in a single strain. As demonstration in a practical application, we use these circuits in two different metabolic engineering examples. We show that bidirectional light control achieved by combining OptoQ-AMP with our original OptoINVRT circuits improves acetoin production compared to unidirectional controls. We also apply bidirectional light control to fine-tune production of geraniol/linalool blend compositions, implicated in the flavor profile of beer. Our findings establish the Q System as a new chemical inducible system for *S. cerevisiae*, which can also be used to develop new optogenetic circuits for practical applications, such as metabolic engineering.

RESULTS AND DISCUSSION

Expression of the *N. crassa* Q System in *S. cerevisiae*. To obtain a functional QF in *S. cerevisiae* (Figure 1a), we expressed a truncated version lacking the middle domain of the protein (residues 206−650) but with N-terminal DNA-binding and C-terminal transcriptional activation domains intact. This truncated version, previously named QF2, was found to alleviate toxicity of QF in *D. melanogaster* without sacrificing transcriptional strength.[17] We also designed a QF2-activated synthetic promoter for *S. cerevisiae* by embedding five QUAS sites within a truncated P_{CYC1} promoter[18] (see Materials and Methods), which we call P_{5xQUAS} (Supporting Information (SI) Sequence S1). Using QF2 (transcribed from P_{PGK1}) to constitutively express green fluorescent protein (GFP) from P_{5xQUAS} achieves the same expression level as the strong constitutive P_{TEF1} promoter (Figure 1b). However, P_{5xQUAS} alone (without expressing QF2), also shows substantial endogenous constitutive activity, reaching 5.8% of P_{TEF1} expression. Furthermore, P_{5xQUAS} activity is enhanced in media containing galactose (SI Figure S1), possibly through the derepression of Gal4p activity. To avoid potential cross-

https://doi.org/10.1021/acssynbio.1c00229
ACS Synth. Biol. XXXX, XXX, XXX−XXX

activation of P_{5xQUAS} by Gal4p, we replaced all CGG sequences (found in Gal4p binding sites) from P_{5xQUAS} with AGG sequences, creating $P_{5xQUASf}$ (SI Sequence S2). We found that $P_{5xQUASf}$ has a 55% and 77% reduction in endogenous constitutive activity compared to P_{5xQUAS} in glucose and galactose, respectively (SI Figure S1), while QF2-mediated activation of this promoter still achieves P_{TEF1} levels of GFP expression (Figure 1b). Thus, $P_{5xQUASf}$ in yeast strains expressing QF2 is a strong constitutive promoter that is not activated by galactose.

We next explored whether QS could repress QF activity in yeast, as it has shown different efficacy levels in other organisms[11,15] (Figure 1a). To test this, we co-expressed QF2 and QS in a strain containing $P_{5xQUASf}$-GFP, using different constitutive promoters of varying strengths[19] to express QS. We found that the extent of QF2 repression depends on the strength of the promoter used to express QS, reaching 74%, 89%, and 98% repression when using P_{ADH1}, P_{HHF2}, and P_{TEF1}, respectively (Figure 1c). These results show that both protein components of the Q System are fully functional in *S. cerevisiae*, and that the transcriptional activity of QF2 is tunable by titrating the expression level of the QS repressor.

Having a functional QF2/QS pair in *S. cerevisiae* offered the possibility of developing a new chemically inducible system in this organism. Quinic acid is known to inhibit QS-mediated repression of QF in *N. crassa*, allowing it to activate transcription of the qa gene cluster[20] (Figure 1a). To test whether we could utilize quinic acid as a new chemical inducer in *S. cerevisiae*, we grew strains containing $P_{5xQUASf}$-GFP, P_{PGK1}-QF2, and QS expressed from different promoters in media containing quinic acid and checked for recovery of GFP expression due to QS inhibition. We observed GFP recovery in strains expressing QS from P_{ADH1} or P_{HHF2} but only after adding >1 g/L quinic acid, and only minimal recovery in the strain expressing QS from P_{TEF1}, likely due to the higher strength of this promoter (SI Figure S2a). Considering the possibility that a quinic acid transport bottleneck was preventing the accumulation of enough intracellular levels to inhibit QS, we added the quinate permease encoded by qa-y from *N. crassa* to the strain expressing QS with P_{HHF2}. The resulting strain shows a 6.6-fold increase in sensitivity to quinic acid: 78% of GFP expression is recovered by addition of 1 mg/L quinic acid, while recovery is above 92% at concentrations >5 mg/L, reaching 96% at 100 mg/L (Figure 1d). Moreover, expression is tunable by varying the concentration of quinic acid between 0.01 and 1 mg/L (SI Figure S2b). We have thus established quinic acid as a new chemical inducer in *S. cerevisiae*, achieving strong gene expression even at low inducer concentrations.

Using the Q System to Develop Optogenetic Inverter (OptoQ-INVRT) Circuits. Although the Q System enables the use of quinic acid as a new alternative to traditional chemical inducers in yeast, it also provides an exogenous platform upon which new optogenetic circuits may be developed. To build inverter circuits based on the Q System, or OptoQ-INVRT circuits, that induce gene expression in the dark, we used VP16-EL222 and P_{C120} to express the QS repressor, thereby repressing QF2 transcriptional activity in blue light while allowing it in the dark (Figure 2a). Guided by the design of our previous OptoINVRT circuits,[4] we used P_{PGK1} to express QF2 and two copies of QS under the control of P_{C120} and VP16-EL222, creating OptoQ-INVRT1. When using OptoQ-INVRT1 to control GFP expression from $P_{5xQUASf}$, we achieve 81.5% of P_{TEF1} expression in darkness compared to 1.3% of P_{TEF1} in blue light or a 61.2-fold induction between light and dark (Figure 2b; see Table 1). In addition, OptoQ-INVRT1 is highly light-sensitive, reaching 99% of full repression when cells are exposed to a 10% light dose (a 10 s ON/90 s OFF light duty cycle). These results show that the Q System can be harnessed to develop new optogenetic circuits with the first demonstration, OptoQ-INVRT1, enabling strong gene expression in the dark and tight repression in the light.

Table 1. OptoQ-INVRT Circuit Characterization

OptoQ-INVRT	1	4
plasmid	pMAL513	pMAL498
strain	yMAL227	yMAL239
QF2 tag	N/A	PSD
QS tag	N/A	ODCmut
fold induction (dark/blue)	61.2	26.5
maximum activation (% P_{TEF1})	81.5	103.2
leakiness (% P_{TEF1})	1.3	3.9
activation in 10/100s blue light (% dark)	3.2	63.0
activation in 1/100s blue light (% dark)	91.3	95.2
half-activation time (hours)	3.2	1.5
time delay (hours)	1.7	<1

We previously showed that our optogenetic inverter circuits exhibit time delays due to the half-life of the repressor protein and that reducing the stability of this repressor leads to faster rates of response and overall enhanced activity of the circuits.[21] Therefore, we set out to improve the activity of OptoQ-INVRT1 by destabilizing QS, which we hypothesized would lead to faster activation kinetics via accelerated derepression of QF2 in the dark (Figure 2c). To achieve this, we integrated two copies of P_{C120}-controlled QS, C-terminally tagged to a weakened variant of the murine ornithine decarboxylase degradation tag (ODCmut).[21] To prevent a potential increase in circuit leakiness under blue light due to reduced QS activity, we also fused a photosensitive degradation tag (PSD)[22] to the C terminus of QF2, which increases its degradation rate in light conditions. The resulting circuit, OptoQ-INVRT4, exhibits a 26.7% increase in the maximum level of GFP expression obtained in the dark, relative to OptoQ-INVRT1, although a 2.9-fold increase in leakiness also reduces the light-to-dark fold of induction to 26.5-fold (Figure 2b; see Table 1). OptoQ-INVRT4 also shows a substantial decrease in light sensitivity, exhibiting a 37% reduction in expression under 10 s ON/90 s OFF light compared to 97% reduction for OptoQ-INVRT1 (Table 1), making OptoQ-INVRT4 easier to fine-tune at intermediate light doses. Therefore, OptoQ-INVRT1 and OptoQ-INVRT4 are both new valuable optogenetic circuits that may be selectively deployed depending on the specific needs for strength, light sensitivity, or fold of induction.

To explore the effect of modifying the half-lives of QF2 and QS on circuit kinetics, we measured the change in GFP expression over time. We found that OptoQ-INVRT1 activation is detectable roughly 1.7 h following induction (switching from light to dark conditions, see Materials and Methods), exhibiting a half-activation time of 3.2 h (Figure 2d; see Table 1, Materials and Methods). The kinetic profile of OptoQ-INVRT1 is similar to that of our fastest previously developed circuit, OptoINVRT7, which employs the Gal80p

https://doi.org/10.1021/acssynbio.1c00229
ACS Synth. Biol. XXXX, XXX, XXX−XXX

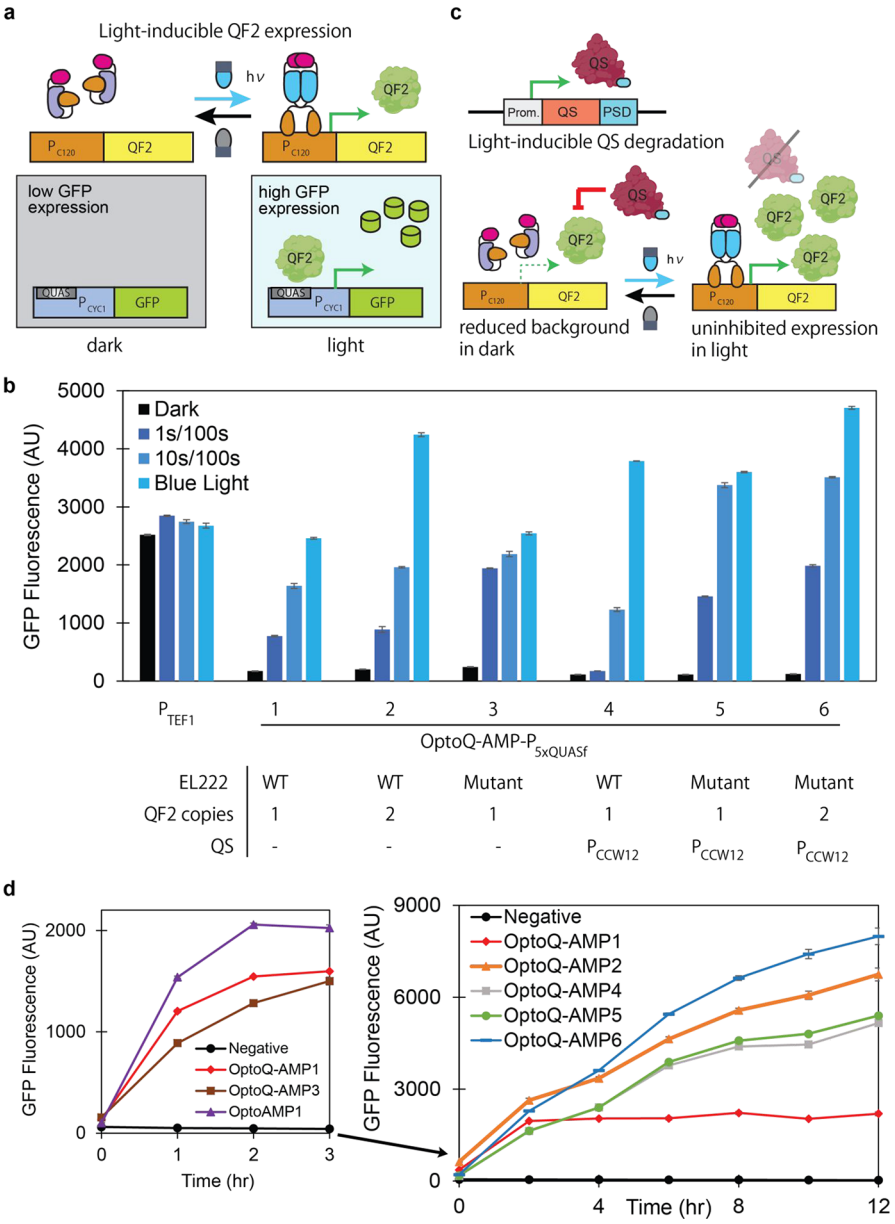

Figure 3. OptoQ-AMP circuit characterization. (a) OptoQ-AMP circuits amplify the transcriptional activity of VP16-EL222 in blue light by transcribing QF2 from the P_{C120} promoter, which then drives high levels of gene expression from the $P_{5xQUASf}$ promoter. (b) GFP expression from P_{TEF1} (YEZ186) or from $P_{5xQUASf}$ controlled by OptoQ-AMP1-6 (yMAL176, yMAL273, yMAL299, yMAL298, yMAL301, yMAL305) under different doses of blue light: full light (100% light), 10 s ON/90 s OFF (10% light), 1 s ON/99 s OFF (1% light), and full darkness (0% light). (c) Addition of QS that is C-terminally tagged with a photosensitive degron (PSD, blue oval) reduces leaky expression in darkness without impeding QF2 activity under blue light. (d) Right panel: time course of GFP expression from $P_{5xQUASf}$ controlled by OptoQ-AMP1 (yMAL176, red diamond), OptoQ-AMP2 (yMAL273, orange triangle), OptoQ-AMP4 (yMAL298, gray square), OptoQ-AMP5 (yMAL301, green circle), and OptoQ-AMP6 (yMAL305, blue dash) compared to a negative control (YEZ140, black circle). Left panel: time course of GFP expression from $P_{5xQUASf}$ controlled by OptoQ-AMP1 (yMAL176, red diamond), OptoQ-AMP3 (yMAL299, brown square), and OptoAMP1 (YEZ72, purple triangle) compared to a negative control (YEZ140, black circle). Strains were grown in darkness until exponential phase (OD_{600} = 1), then switched to full blue light at t = 0. All data shown as median values of 10 000 single-cell flow cytometry events; error bars (often smaller than graphical icons) represent one standard deviation of replicates exposed to the same conditions (n = 3 biologically independent samples). QF2 and QS proteins in (a) and (c) were created with Biorender.com.

repressor and Gal4p activator modified with the same ODCmut and PSD tags, respectively.[21] In contrast, OptoQ-INVRT4 shows a 1.5 h half-activation time (2.5 h faster than OptoINVRT7) and <1 h time delay. In addition, OptoQ-INVRT1 and OptoQ-INVRT4 show tight blue light repression for the duration of the time course (SI Figure S3a). Therefore, modifying the turnover rates of QF2 and QS makes OptoQ-INVRT4 the fastest optogenetic inverter circuit we have developed.

Using the Q System to Develop Optogenetic Amplification (OptoQ-AMP) Circuits. Optogenetic amplification circuits provide another strategy to overcome potential limitations in light penetration, while enabling the use of light-activated systems to control gene expression. We applied the Q System to design new optogenetic amplifier circuits, following

https://doi.org/10.1021/acssynbio.1c00229
ACS Synth. Biol. XXXX, XXX, XXX−XXX

Table 2. OptoQ-AMP Circuit Characterization

OptoQ-AMP	1	2	3	4	5	6
plasmid	pMAL358	pMAL669	pMAL722	pMAL716	pMAL724	pMAL728
strain	yMAL176	yMAL273	yMAL299	yMAL298	yMAL301	yMAL305
EL222	WT	WT	A79Q	WT	A79Q	A79Q
# of QF2	1	2	1	1	1	2
QS_PSD promoter	N/A	N/A	N/A	P_{CCW12}	P_{CCW12}	P_{CCW12}
fold induction (blue/dark)	13.2	19.8	9.9	32.1	30.6	36.9
maximum activation (% P_{TEF1})	91.8	158.5	95.0	141.6	134.5	175.8
leakiness (% P_{TEF1})	6.8	8.0	9.6	4.4	4.4	4.8
Activation in 10/100s blue light (% full blue)	65.0	45.0	83.9	31.7	91.4	72.8
activation in 1/100s blue light (% full blue)	29.7	19.6	71.8	4.3	38.0	39.7

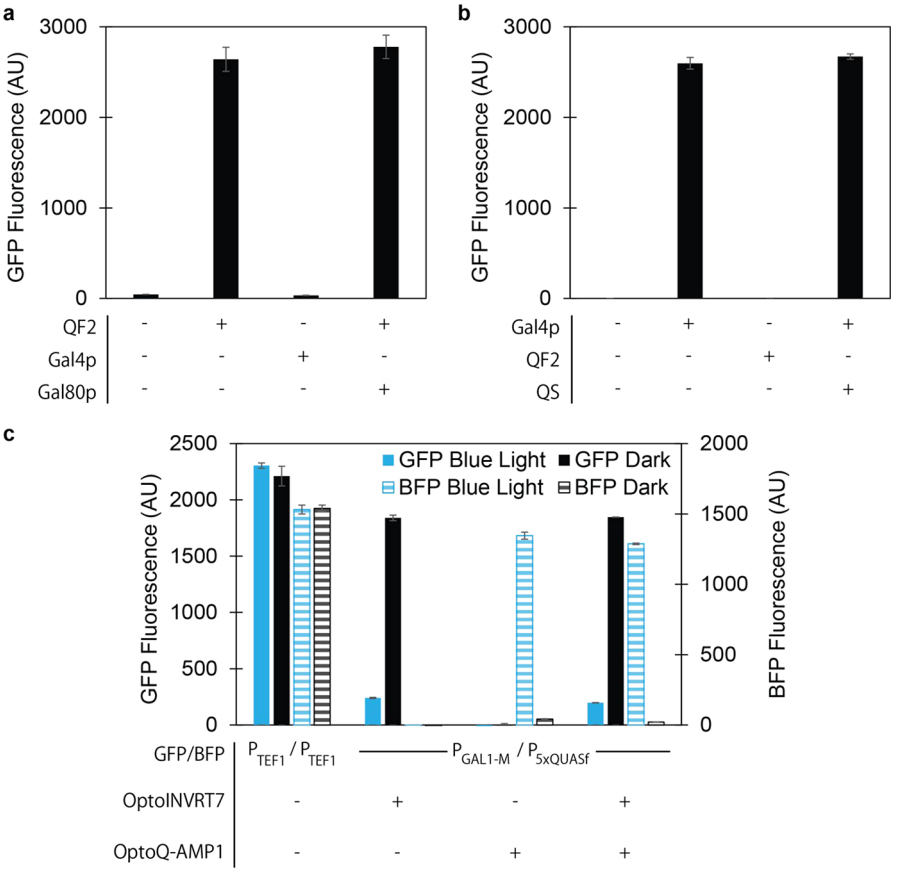

Figure 4. GAL and Q System orthogonality. (a) GFP expression from $P_{5xQUASf}$ by itself (yMAL207) with QF2 (yMAL268), with Gal4p (yMAL195), or with QF2 and Gal80 (yMAL198). (b) GFP expression from P_{GAL1} by itself (YEZ82), with constitutive Gal4p (yMAL194), with QF2 (yMAL251), or with constitutive Gal4p and QS (yMAL197). (c) GFP and BFP expression from P_{TEF1} (yMAL270), GFP expression from P_{GAL1-M} controlled by OptoINVRT without BFP expression (yMAL245), BFP expression from $P_{5xQUASf}$ controlled by OptoQ-AMP1 without GFP expression (yMAL249), and GFP expression from P_{GAL1-M} controlled by OptoINVRT and BFP expression from $P_{5xQUASf}$ controlled by OptoQ-AMP1 (yMAL246), under different doses of blue light: full light (100% light), 10 s ON/90 s OFF (10% light), 1 s ON/99 s OFF (1% light), and full darkness (0% light). All data shown as median values of 10 000 single-cell flow cytometry events; error bars represent one standard deviation of replicates exposed to the same conditions (n = 3 biologically independent samples).

a similar architecture as our previously developed OptoAMP circuits, which are based on the GAL regulon.[5] We used VP16-EL222 to control QF2 from P_{C120}, making its expression, and thus expression of genes downstream of $P_{5xQUASf}$, blue light-inducible (Figure 3a). This circuit, which we call OptoQ-AMP1, can amplify the effective transcriptional response of VP16-EL222 (direct activation with OptoEXP circuit[4,5]) by 8.9-fold, reaching 92% of P_{TEF1}-GFP expression levels under full blue light, compared to 6.8% of P_{TEF1} in the dark (Figure 3b and SI Figure S4). OptoQ-AMP1 exhibits a 13.5-fold induction between light and darkness with intermediate levels of expression under shorter light duty cycles. To increase the maximum expression levels, we added an extra copy of P_{C120}-QF2, resulting in OptoQ-AMP2, which achieves 158% the expression levels of P_{TEF1} in blue light, and a 19.8-fold dark-to-light induction. Furthermore, to increase light sensitivity, we used a mutant EL222 (A79Q), which has an increased lit-state half-life of 300 s compared to 30 s of the wild-type.[23] The resulting circuit, OptoQ-AMP3, is highly sensitive to light, reaching 72% of maximum activation with only 1% light dose

https://doi.org/10.1021/acssynbio.1c00229
ACS Synth. Biol. XXXX, XXX, XXX−XXX

(a 1 s ON/99 s OFF light duty cycle). While these modifications improve the strength and sensitivity of OptoQ-AMP circuits, they also increase their leakiness in the dark (7.9% and 9.6% of P_{TEF1}, for OptoQ-AMP2 and OptoQ-AMP3, respectively; see Table 2), so we aimed to further engineer the circuits to reduce background expression.

To preserve tight repression in the OFF-state without sacrificing ON-state expression, we coexpressed the QS repressor C-terminally tagged with a PSD.[24] With this modification, QS stably represses leaky expression from QF2 in the dark but is rapidly degraded under blue light to preserve maximal expression (Figure 3c). To find an optimal expression level for QS-PSD, we tested a range of constitutive promoters (from weaker to stronger: P_{RNR2}, P_{PGK1}, and P_{CCW12}[19]). Higher QS-PSD expression levels (P_{PGK1} and P_{CCW12}) reduce leaky gene expression in the dark as expected, but also increase gene expression under full light, a similar phenomenon to what we observe in our OptoQ-INVRT4 inverter circuit (SI Figure S5). On the basis of this finding, we expressed QS-PSD from the strong P_{CCW12} promoter alongside one copy of P_{C120}-QF2. This new circuit, OptoQ-AMP4, shows lower basal expression in the dark (4.4% of P_{TEF1}) and higher expression in full light (142% of P_{TEF1}) compared to OptoQ-AMP1 (Figure 3b). Because OptoQ-AMP4 exhibits reduced light sensitivity, we replaced EL222 with the hypersensitive $EL222^{A79Q}$ variant to make OptoQ-AMP5, which shows an 8.4-fold increase in activation under 1% light exposure. Finally, we added an extra copy of P_{C120}-QF2 to OptoQ-AMP5, creating OptoQ-AMP6, which shows the highest activation levels (176% of P_{TEF1} under full light) and largest dynamic range (37-fold induction) of our OptoQ-AMP circuits (Figure 3b; see Table 2). The differences observed in strength, sensitivity, tunability, and fold of induction between this suite of OptoQ-AMP circuits, provide flexible options for the particular needs of different applications.

We also characterized the response times of our OptoQ-AMP circuits by measuring changes in GFP expression over time after switching strains from darkness to full light. OptoQ-AMP1 and OptoQ-AMP3 exhibit similar kinetics to those of our previously developed OptoAMP1 circuit,[5] reaching 78% of maximum GFP expression in 1 h and full expression within 3 h of light induction (Figure 3d). Moreover, the additional copy of QF2 (in OptoQ-AMP2 and 6) and/or QS-PSD (in OptoQ-AMP4, 5, and 6) significantly increases maximum expression capacity while maintaining similar initial activation kinetics. While the simpler OptoQ-AMP1, OptoQ-AMP3, and Opto-AMP1 reach full activation within 3 h, circuits containing QS-PSD or an extra copy of QF2 (OptoQ-AMP2, 4, 5, and 6) continue to induce expression for at least 9 h more, which allows them to achieve higher levels of gene expression (Figure 3d; see Table 2). Furthermore, fold-changes between light and darkness remain high 12 h after induction, indicating tight OFF-state control (SI Figure S3b). Therefore, all OptoQ-AMP circuits show rapid initial activation rates with the strongest ones (OptoQ-AMP2, 4, 5, and 6) exerting their effect over longer periods of time.

The Q System Is Orthogonal to the GAL Regulon. To combine inverter and amplifier circuits in a single strain, it is necessary to use orthogonal circuit components. Because the original P_{5xQUAS} promoter showed higher activity in galactose media, we explored whether the GAL and Q Systems exhibit crosstalk by examining if each system affects the gene expression driven by the other. Using GFP as a reporter, we found that constitutive expression of *GAL4* does not activate $P_{5xQUASf}$, while coexpressing *GAL80* with QF2 does not reduce GFP expression compared to expressing QF2 alone (Figure 4a). These results confirm that Gal4p and Gal80p do not interfere with the activities of $P_{5xQUASf}$ or QF2. Similarly, constitutive expression of QF2 does not activate P_{GAL1}, and coexpression of *GAL4* and QS does not decrease gene expression relative to expressing *GAL4* alone (Figure 4b). These results demonstrate that Gal4p and Gal80p do not interfere with the activities of $P_{5xQUASf}$ or QF2, and similarly QF2 and QS do not interfere with P_{GAL1} or Gal4p. The robust orthogonality between the GAL regulon and Q System thus allows for application of optogenetic signal amplification and inversion in the same strain.

To confirm that we could simultaneously use our optogenetic amplifiers and inverters without cross-interference, we integrated in a single strain both OptoINVRT7 to control GFP expression from $P_{GAL1\text{-}M}$, and OptoQ-AMP1 to control expression of the blue fluorescent protein mTagBFP2 (BFP) from $P_{5xQUASf}$. We also made control strains containing both OptoINVRT7 and OptoQ-AMP1 but only either GFP or BFP. When we cultured these strains in darkness and blue light, we found that GFP expression from OptoINVRT7 is unaffected by the presence of OptoQ-AMP1 driving BFP, and vice versa, expression of BFP in the light is unchanged by OptoINVRT7 (Figure 4c). The fact that there is no reduction in maximal expression of GFP (from OptoINVRT7) or BFP (from OptoQ-AMP1) suggests that intracellular levels of VP16-EL222 (which is expressed from the strong P_{TEF1} promoter) are not limiting even when controlling two optogenetic circuits. Our results confirm that our amplifier and inverter circuits function orthogonally in the same strain, opening the door for their simultaneous use in practical applications, such as metabolic engineering for chemical production.

Simultaneous Optogenetic Amplification and Inversion for Chemical Production. To demonstrate the benefit of implementing amplifier and inverter circuits simultaneously in a single strain, we applied them to metabolic engineering, co-utilizing OptoQ-AMP and OptoINVRT circuits to respectively control cellular growth and the biosynthetic pathway for a chemical of interest. In *S. cerevisiae* fermentations, pyruvate decarboxylases (Pdc enzymes encoded by *PDC1*, *PDC5*, and *PDC6*) compete with metabolic pathways of interest that utilize pyruvate, producing ethanol as an undesirable fermentation byproduct. However, deleting all three *PDC* genes results in strains that are unable to grow on glucose.[25] To overcome this challenge, we used OptoQ-AMP1 to control the expression of *PDC1* from $P_{5xQUASf}$ in a Pdc-deficient (*pdc1*, *pdc5*, *pdc6*) strain, resulting in strain yMAL241. With this optogenetic amplifier, a single copy of *PDC1* is sufficient to recover growth on glucose, even at light doses as low as 10% (100 s ON/900s OFF duty cycles) (SI Figure S6). This contrasts with previous similar light-dependent strains obtained without amplification (using VP16-EL222 in the direct OptoEXP circuit), which require six copies of *PDC1* driven by P_{C120} and full light to grow on glucose.[4] Although this new light-dependent strain exhibits a longer lag phase, there is no reduction in biomass accumulation compared to a wild-type control. OptoQ-AMP1 thus provides sufficient transcriptional amplification to optogenetically control growth of Pdc-deficient yeast using a single copy of *PDC1*.

https://doi.org/10.1021/acssynbio.1c00229
ACS Synth. Biol. XXXX, XXX, XXX−XXX

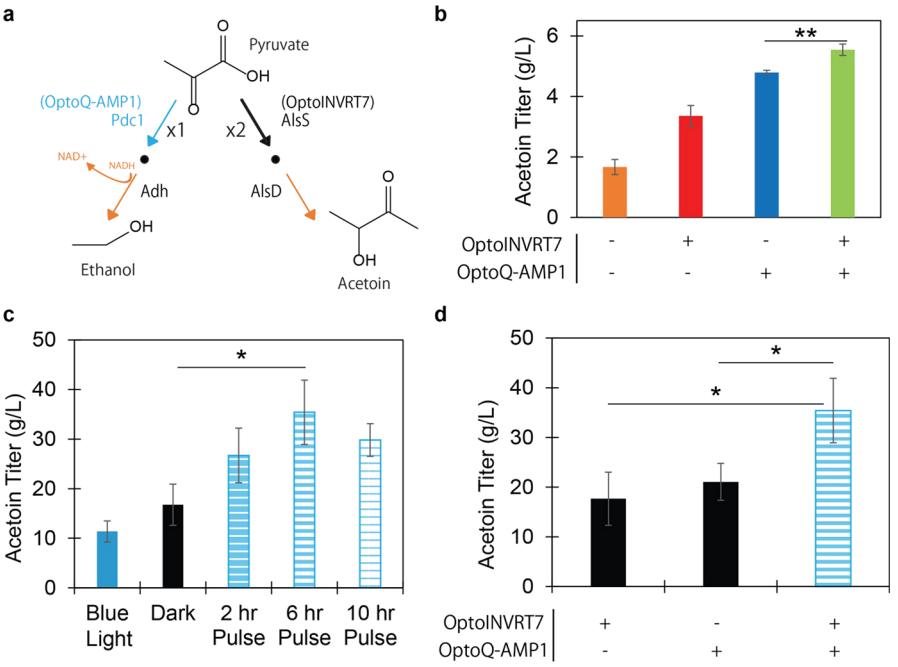

Figure 5. Acetoin production using OptoQ-AMP and OptoINVRT7. (a) Metabolic branch point between ethanol (Pdc1p) and acetoin (AlsS) production. *PDC1* is expressed from $P_{5xQUASf}$ controlled by OptoQ-AMP1 in blue light (blue arrow); *alsS* (from *B. subtilis*) is expressed from $P_{GAL1\text{-}S}$ controlled by OptoINVRT7 in darkness (black arrow). Orange arrows represent endogenous expression (*adh*) or constitutive expression from P_{CCW12} (*alsD* from *B. subtilis*). (b) Acetoin production in fermentations of 48 h and 20 g/L glucose when constitutively expressing endogenous *PDC1* and *alsS* from P_{TDH3} (yMAL364, orange); expressing endogenous *PDC1* and *alsS* from $P_{GAL1\text{-}S}$ controlled by OptoINVRT7, using $\rho_s = 0.2$ (yMAL332, red); expressing *PDC1* from $P_{5xQUASf}$ controlled by OptoQ-AMP1 and *alsS* from P_{TDH3}, using $\rho_s = 0.3$ (yMAL323, blue); or expressing *PDC1* from $P_{5xQUASf}$ controlled by OptoQ-AMP1 and *alsS* from $P_{GAL1\text{-}S}$ controlled by OptoINVRT7, using $\rho_s = 0.5$ (yMAL322, green). (c) Acetoin production in fermentations of 96 h and 150 g/L glucose using $\rho_s = 0.5$ for yMAL322. During the production phase (following resuspension in fresh media), cultures were incubated in full blue light for 4 h, then subjected to light duty cycles of 10 s ON/90 s OFF (10% light) for 30 min every 2, 6, or 10 h. Control cultures were kept in blue light or darkness for the entire production phase. (d) Acetoin production in fermentations of 96 h and 150 g/L glucose using $\rho_s = 0.5$ and a duty cycle of 10 s ON/90 s OFF (10% light) for 30 min every 6 h during the production phase for yMAL322; $\rho_s = 0.3$ and full darkness during the production phase for yMAL323; or $\rho_s = 0.2$ and full darkness during the production phase for yMAL332. For each strain, Zeocin (1200 μg/mL) was used to select for multicopy integration of the acetoin pathway, and the highest producing colony from an initial screen ($n = 8$) was selected for subsequent analysis. *$P < 0.05$, **$P < 0.01$. Statistics are derived using a two-sided *t*-test. All data shown as mean values; error bars represent one standard deviation of replicates exposed to the same conditions ($n = 4$ (b) or $n = 3$ (c, d) biologically independent samples).

Using OptoINVRT7, we then set out to redirect pyruvate in yMAL241 toward the biosynthesis of a desired chemical during a darkness-induced production phase. We demonstrate this capability for the production of acetoin, a desired food flavoring agent known for its buttery odor, whose biosynthetic pathway directly competes for pyruvate with ethanol production. We integrated into δ-sites[26] of yMAL241 a construct containing two enzymes from *Bacillus subtilis* that convert pyruvate to acetoin:[27] α-acetolactate synthase (*alsS*) under the control of the P_{GAL1} hyperactive derivative $P_{GAL1\text{-}S}$[21] which makes it dark-inducible with OptoINVRT7, and α-acetolactate decarboxylase (*alsD*) constitutively expressed with P_{CCW12} (Figure 5a; see Materials and Methods), naming the resulting strain yMAL322. As controls, we also made strains with a light-inducible *PDC1* but a constitutively expressed acetoin pathway (controlling growth only), an endogenous *PDC1* but a dark-inducible acetoin pathway (controlling production only), and an endogenous *PDC1* and a constitutively expressed acetoin pathway (controlling neither growth nor production). To compare acetoin production in each optogenetically controlled strain, we optimized the cell density at which cultures are switched from growth to production (ρ_s)[4] (SI Figure S7). For all three strains, acetoin production is maximized at relatively low ρ_s values ($\rho_s = 0.2$–0.5). Strain yMAL322, using both OptoQ-AMP1 and OptoINVRT7, achieves the highest maximum titers of the three, with 5.5 ± 0.2 g/L, while the strain using only OptoINVRT7 to control *alsS* achieves the lowest with 3.4 ± 0.3 g/L (SI Figure S7). Therefore, using amplifier and inverter circuits simultaneously to dynamically controlling both cell growth (*PDC1*) and acetoin biosynthesis (*alsS*) results in the highest acetoin production. This is demonstrated by yMAL322 achieving 232% higher titers than a strain without growth or production control, which is also higher than titers obtained from strains controlling only growth (with OptoQ-AMP1) or only production (with OptoINVRT7) by 16% and 65%, respectively (Figure 5b). For this metabolic branch point, regulating growth (*PDC1*) appears to be more critical than regulating production (*alsS*), as indicated by comparing acetoin production in strains using only one optogenetic circuit. Nevertheless, controlling both growth and production leads to the highest production, demonstrating the value in using simultaneous amplification and inversion of optogenetic responses, specifically in this case, in metabolic engineering for chemical production.

The ability to tune gene expression without manipulating process conditions or media components makes light an attractive option for inducing gene expression. We previously

https://doi.org/10.1021/acssynbio.1c00229
ACS Synth. Biol. XXXX, XXX, XXX−XXX

showed that pulsing light during the production phase of a fermentation could restore NAD^+ levels through transient *PDC1* expression, thus preventing premature metabolic arrest and improving isobutanol titers.[4] Therefore, we set out to determine if simultaneous optogenetic amplification and inversion could enhance the effect of this strategy to boost acetoin production, whose biosynthesis also results in an NAD^+/NADH imbalance. We carried out light-controlled fermentations in synthetic complete medium with 15% glucose and light-pulsed production phases using yMAL322, containing both OptoQ-AMP1 and OptoINVRT7 (to control growth and production, respectively), as well as control strains containing only one of each circuit. We incubated the cultures under continuous light stimulation during the growth phase until the optimal ρ_s value was reached for each strain (SI Figure S7). Following a 2 h incubation in the dark, we pelleted and resuspended cells in fresh media, then started a production phase in which different light schedules were applied (see Materials and Methods). Periodic light pulses during the production phase do not increase acetoin production in strains containing only OptoQ-AMP1 or OptoINVRT7 relative to their production in full darkness (21 ± 4 and 18 ± 5 g/L, respectively) (SI Figure S8). In contrast, acetoin titers increase up to 111% in yMAL322 using light pulses compared to its production in full darkness; while acetoin production reaches 17 ± 4 g/L in full darkness, it achieves 35 ± 6 g/L when using a 10 s ON/90 s OFF duty cycle (10% light dose) for 30 min every 6 , during the 96-h production phase (Figure 5c). This maximum titer achieved by yMAL322 is 68% and 100% higher than those reached by strains containing only OptoQ-AMP1 or OptoINVRT7 in full darkness, respectively (Figure 5d). These results thus demonstrate that simultaneous amplification and inversion of metabolic optogenetic responses can boost the production benefits of periodically operating light-responsive fermentations with light pulses.

Simultaneous Optogenetic Amplification and Inversion to Fine-Tune Enzyme Levels. As a second demonstration of the utility of optogenetic bidirectional control, we combined optogenetic amplifier and inverter circuits to achieve a delicate balance of metabolic pathways that carry lower fluxes. These circuits can fine-tune the production levels of different proteins by varying light exposure. For example, expression levels of two fluorescent proteins (GFP and BFP) in the same strain can be tuned using different light duty cycles with a 10% light dose (10 s ON/90 s OFF duty cycle) resulting in intermediate levels of both GFP and BFP expression (Figure 6a). Thus, we reasoned that such control could be extended to biosynthetic enzymes for fine-tuning blends of chemicals in which composition is more important than final titers. To test this hypothesis, we applied our OptoINVRT7 and OptoQ-AMP4 circuits to simultaneously regulate the biosyntheses of geraniol and linalool, two monoterpenes implicated as primary contributors to the hoppy flavor in beer. In a previous study, a combinatorial expression library was used to generate strains of brewer's yeast with different levels of geraniol and linalool production, from which beer of desired flavor profiles could be achieved.[28] By controlling geraniol production with an optogenetic amplifier circuit and linalool production with an inverter circuit, we sought to instead apply different light pulses to adjust the composition of these hoppy flavor monoterpenes in fermentations using a single strain.

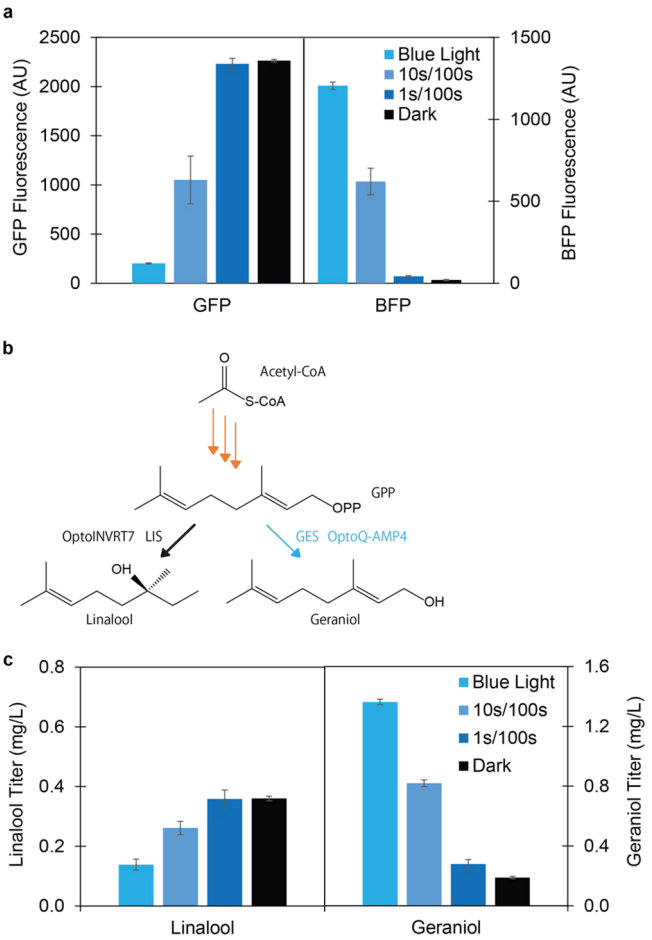

Figure 6. Geraniol and Linalool production tunability using OptoQ-AMP and OptoINVRT7. (a) GFP expression from $P_{GAL1\text{-}M}$ controlled by OptoINVRT7 and BFP expression from $P_{5xQUASf}$ controlled by OptoQ-AMP1 in a single strain (yMAL246) under different doses of blue light: full light (100% light), 10 s ON/90 s OFF (10% light), 1 s ON/99 s OFF (1% light), and full darkness (0% light). (b) Metabolic branch point between geraniol (ObGES) and linalool (McLIS) production. ObGES is expressed from $P_{5xQUASf}$ controlled by OptoQ-AMP4 (blue arrow) and McLIS is expressed from $P_{GAL1\text{-}S}$ controlled by OptoINVRT7 (black arrow). Orange arrows represent endogenous expression of the mevalonate pathway and constitutive expression of $ERG20^{F96C}$ from P_{TDH3}. (c) Tunability of geraniol and linalool production using both OptoINVRT7 and OptoQ-AMP1 in the same strain (yMAL360) under different doses of blue light: full light (100% light), 10 s ON/90 s OFF (10% light), 1 s ON/99 s OFF (1% light), and full darkness (0% light). All data shown as mean values; error bars represent one standard deviation of replicates exposed to the same conditions (n = 3 (a) or n = 4 (c) biologically independent samples).

To balance geraniol and linalool production with light, we used OptoQ-AMP4 to control the expression of geraniol synthase from *Ocimum basilicum* (ObGES) from $P_{5xQUASf}$, as well as OptoINVRT7 to control the expression of linalool synthase from *Mentha citrata* (McLIS) from $P_{GAL1\text{-}S}$ (Figure 6b). The resulting strain, yMAL360, can produce blends of different compositions of geraniol and linalool depending on the light duty cycles to which the fermentation is exposed, favoring geraniol production with increasing light doses, and linalool with longer periods of darkness (Figure 6c). Linalool production saturates at lower light duty cycles (1 s ON/99 s OFF), reaching maximum titers of 0.36 ± 0.01 mg/L. In contrast, geraniol concentrations remained tunable within the

https://doi.org/10.1021/acssynbio.1c00229
ACS Synth. Biol. XXXX, XXX, XXX−XXX

range of light-duty cycles tested, reaching as much as 1.4 ± 0.1 mg/L in full light. These results imply that McLIS has lower catalytic activity than ObGES, given that the level of expression achieved with OptoINVRT7 using $P_{GAL1\text{-}S}$ is 2.5-fold that of P_{TEF1},[21] while OptoQ-AMP4 achieves 1.4-times P_{TEF1} levels. Higher linalool production could likely be attained by using a mutant LIS with higher activity,[29] adding an N-terminal SKIK tag to improve expression,[30] or introducing additional copies of LIS. Nevertheless, the ability to use light to fine-tune the composition of geraniol-linalool blends in a single strain demonstrates the vast potential of combining optogenetic amplifier and inverter circuits to balance metabolic pathways, whether they carry high or low metabolic fluxes.

CONCLUSION

In this study, we have developed and characterized the Q System as a heterologous system for transcriptional regulation in *S. cerevisiae*. While the Q System has been implemented in several other model organisms and cell lines, it is often not a trivial task, having not all of its components necessarily function as expected (if at all) in heterologous hosts. For example, quinic acid enhances rather than inhibits QS activity in mammalian cells[11] and is toxic at >0.5 mg/mL concentrations in zebrafish.[13] Additionally, QS does not function in CHO cells,[15] has not been characterized in mosquitoes,[14] and requires >3 copies to effectively repress QF in *D. melanogaster* and HeLa cells.[11] In contrast, we have established the proper functionality of all three Q System components (QF2, QS, and quinic acid) in *S. cerevisiae* with low gene copy number (QF2, QS) and quinic acid concentration requirements, allowing for its robust and versatile use as a chemically or optogenetically inducible system.

As a chemical inducer, quinic acid has several advantages over existing agents. It achieves full induction (derepression of QF2) at extracellular concentrations as low as 5 mg/L, provided the qa-y transporter is expressed (Figure 1d). In addition, quinic acid has not been detected as a native metabolite in *S. cerevisiae*, suggesting it can be used as a chemical inducer without concerns of cross-talk with native metabolic pathways, unlike the use of galactose, ethanol, copper, or methionine to control gene expression. Simply adding quinic acid to fermentation media is also an advantage over the media replacements required for nutrient- or carbon-source-based inducers, which can be cumbersome, slow, and cause metabolic side effects. Finally, quinic acid is less expensive than commonly used chemical inducers such as doxycycline and β-estradiol, making it more amenable to scaleup. These advantages make quinic acid a useful new chemical inducing agent for dynamic regulation of *S. cerevisiae* gene expression.

Another key advantage of the Q System is its orthogonality with the endogenous GAL regulon. The transcriptional activators of the Q System and GAL regulon (QF2 and Gal4p) do not activate each other's promoters ($P_{5xQUASf}$ and P_{GAL1}), and their repressors (QS and Gal80p) do not inhibit each other's activators, making them tightly orthogonal. Thus, the Q System and GAL regulon could be applied to chemically control different cellular functions simultaneously in yeast. Additionally, the basic architectures of these systems share enough similarities that the same circuit designs can be used to develop optogenetic amplifiers and inverters from each of them, which also remain tightly orthogonal. This allows the simultaneous deployment of these optogenetic circuits in the same strain, which enables the effective use of both light[5] as well as darkness[4,21] to achieve bidirectional control of different sets of genes in high cell density fermentations. Using both circuits, as opposed to only one, to control growth (*PDC1*) and production (*alsS*) proved to be advantageous in acetoin production (Figure 5). Production could be further improved by previously described interventions, such as deleting additional alcohol and glycerol-3-phosphate dehydrogenases, or overexpressing NADH oxidase,[27] as well as by implementing optimized fed-batch fermentations with richer media, pH and aeration controls, and glucose feeding. Nevertheless, the goal of this study is to provide a proof of principle that the dynamic bidirectional control achieved with simultaneous optogenetic amplification and inversion could improve the productivity of biosynthetic pathways that compete with essential metabolism. The ability of this simultaneous dual optogenetic function to control monoterpene blend composition demonstrates that these systems can also be used to fine-tune metabolic pathways to maintain a delicate balance of different intermediate metabolites. These capabilities could be extended to control the composition of other product blends (e.g., branched-chain alcohols in biofuel blends[31,32]) or key metabolic intermediates (e.g., phosphoenolpyruvate and erythrose-4-phosphate to better produce shikimate pathway derivatives[33]). Therefore, the orthogonality of the optogenetic circuits derived from the Q System and GAL regulon expand the applicability of optogenetics in metabolic engineering by facilitating the use of light to control diverse metabolic branch points.

Both OptoQ-INVRT and OptoQ-AMP circuits provide strong and prolonged gene expression (in darkness or minimal light, respectively) as well as rapid activation kinetics. All OptoQ-circuits activate within 1 or 2 h of induction, which compares favorably with our fastest optogenetic circuits.[21] Additional copies of QF2 or expression of PSD further extend the level of amplification of OptoQ-AMP circuits even after 12 h (Figure 2d), likely due to increased levels of QF2-mediated signal amplification and possible alterations of QS activity by the PSD tag. The enhanced light sensitivity and duration of activation provided by OptoQ-AMP circuits hold promise for robust light-induced activation during the growth phase of larger-scale fermentations, which we have already demonstrated using earlier circuit designs.[4,5] On the other hand, OptoQ-INVRT circuits are stronger and faster (especially OptoQ-INVRT4) than the GAL regulon-based OptoINVRT7, the fastest optogenetic circuit we had previously developed.[21] The enhanced kinetics of OptoINVRT7 requires engineered destabilization of the Gal80p repressor, suggesting that QS is inherently less stable in *S. cerevisiae*, probably because of its heterologous nature. Using darkness to induce the production phase, combined with using amplifier circuits to achieve higher gene expression levels under blue light, can address potential light penetration limitations in larger bioreactors. In general, there are many potential solutions to address limited light penetration, such as developing light-controlled circuits with enhanced activation strengths and sensitivities (as in this study), as well as designing photobioreactors with higher illumination capabilities.[34,35] The differences in time scales of activation between OptoQ-INVRT4 (<2 h) and first-generation OptoINVRT circuits (>9 h) could potentially be leveraged to develop semi-orthogonal controls for different sets of genes,[36] using specific light schedules that keep the rapid

https://doi.org/10.1021/acssynbio.1c00229
ACS Synth. Biol. XXXX, XXX, XXX−XXX

circuit (OptoQ-INVRT4) activated, while the slower circuit (e.g. OptoINVRT1) is off. In this sense, our "faster" OptoQ-INVRT circuits could be useful both for their quickness of activation and for their kinetic separation from our "slower" OptoINVRT circuits. Altogether, the favorable kinetics of OptoQ circuits is an important advantage that will help realize the full potential of optogenetics for different biotechnological applications, including metabolic engineering.[37]

The orthogonality of the Q System could be extended to develop multichromatic controls of gene expression. Gal4p has previously been split into its DNA-binding and transactivation domains, then paired with plant or bacterial phytochromes and their interacting factors, systems which are responsive to red and far-red wavelengths of light, to achieve red light-controlled gene expression.[38−41] Because these systems employ Gal4p-activated promoters, they are not compatible with our GAL regulon-based OptoINVRT and OptoAMP systems. However, they could be used in combination with our OptoQ-AMP and OptoQ-INVRT circuits to control separate sets of genes using both red/far-red and blue wavelengths of light, respectively. Thus, the Q System thus provides additional avenues for developing gene circuits that respond orthogonally to different wavelengths of light.

The Q System provides a new chemical inducer (quinic acid) for control of gene expression, as well as a robust and flexible set of optogenetically inducible systems to both optimize and fine-tune gene expression in yeast. The ability to co-utilize amplifier and inverter circuits for bidirectional transcriptional controls with wide dynamic ranges and rapid activation kinetics bodes well for controlling key metabolic valves and other key functional genes with both quickness and precision. These capabilities, coupled with future implementation of optogenetic systems triggered by orthogonal wavelengths and light pulse scheduling,[42] provide a strong foundation for the development of dynamic, multiplexed, and eventually automated, control of yeast for chemical production and beyond.

MATERIALS AND METHODS

Plasmid and Strain Construction. We cloned promoter-gene-terminator sequences into standardized vector series (pJLA vectors[43]) as previously described[4] (SI Table S1 and SI Figure S9). When pJLA vectors were not available, we used Gibson isothermal assembly[44] to insert constructs into pJLA vectors for compatibility with the rest of our vectors. Epoch Life Science DNA Miniprep, Omega E.Z.N.A. Gel Extraction, and Omega E.Z.N.A. Cycle Pure kits were used to extract and purify plasmids and DNA fragments. Genes and promoters (*GAL4*, *GAL80*, GFP, $P_{GAL1\text{-}M}$, $P_{GAL1\text{-}S}$, P_{CCW12}, P_{TEF1}, P_{PGK1}, P_{HHF2}, P_{ADH1}, P_{RNR2}) were amplified from yeast genomic DNA or lab plasmids, using CloneAmp HiFi PCR premix from Takara Bio, following manufacturer's instructions. Primers were ordered from Integrated DNA Technologies (Coralville, IA). All plasmids were verified using Sanger sequencing from Genewiz (South Plainfield, NJ). We avoid using tandem repeats to prevent recombination after transformation and thus do not observe instability of strains.

The QF2, QS, qa-y, and P_{5xQUAS} sequences were synthesized by Bio Basic's gene synthesis service. The $P_{5xQUASf}$ sequence was synthesized by Synbio Technologies' gene synthesis service. To make P_{5xQUAS} (SI Sequence S1), we placed five QUAS binding sites upstream of the TATA-1β box of a truncated 209-base-pair P_{CYC1} promoter with UAS1 and UAS2 sites removed.[18] Because the original 5xQUAS sequence contains a CGG-N_{12}−CGG sequence, which is similar to the CGG-N_{11}−CGG sequence recognized by Gal4p, we replaced all CGG sequences with AGG sequences to prevent potential activation of the promoter by Gal4p, calling this variant $P_{5xQUASf}$ (SI Sequence S2).

Yeast transformations were carried out using standard lithium acetate protocols;[45] the resulting strains are catalogued in SI Table S2. Gene deletions (*BDH1*) were carried out by homologous recombination as previously described.[4] Gene assemblies in pYZ12-B, pYZ162, and pYZ23 were integrated into the *HIS3* locus, *LEU2* locus, or δ-sites (YARCdelta5) as previously described.[5] Zeocin (Thermo Fisher Scientific) was used at a concentration of 1200 μg/mL to select for δ-integration.

Yeast Cell Culture Growth, Centrifugation, and Optical Measurements. Single colonies from agar plates were inoculated into liquid SC dropout media in triplicate and grown in 96-well (U.S.A. Scientific #CC7672-7596) or 24-well (U.S.A. Scientific #CC7672-7524) plates at 30 °C and shaken at 200 rpm (19 mm orbital diameter). To stimulate cells with blue (465 nm) light, we used LED panels (HQRP New Square 12" Grow Light Blue LED 14W) placed above the culture such that light intensity was between 80 and 110 μmol/m^2/s as measured using a Quantum meter (Apogee Instruments, Model MQ-510), which corresponds to placing the LED panels approximately 40 cm from the cultures. To control light duty cycles, LED panels were regulated with a Nearpow Multifunctional Infinite Loop Programmable Plug-in Digital Timer Switch.

To measure cell concentration, optical density measurements were taken at 600 nm (OD_{600}), using media (exposed to the same light and incubation conditions as the yeast cultures) as blank. Measurements were taken using a TECAN plate reader (infinite M200PRO) or Eppendorf spectrophotometer (BioSpectrometer basic) with a microvolume measuring cell (Eppendorf μCuvette G1.0), using samples diluted to a range of OD_{600} between 0.1 and 1.0.

Flow Cytometry. GFP fluorescence was quantified by flow cytometry using a BD LSR II flow cytometer and BD FacsDiva 8.0.2 software (BD Biosciences, San Jose, CA, U.S.A.) with a 488 nm laser and 525/50 nm bandpass filter. BFP fluorescence was quantified with a 405 nm laser and 450/50 nm bandpass filter. For experiments involving both GFP and BFP, compensation was applied to account for spectral overlap. The gating used in our analyses was defined to include positive (YEZ186 for GFP; yMAL270 for GFP + BFP) and negative (YEZ140; yMAL248) cells based on fluorescence (SI Figure S10a,b) but exclude particles that are either too small or too large to be single living yeast cells, based on the side scatter (SSC-A) versus forward scatter (FSC-A) plots as well as forward scatter area (FSC-A) versus width (FSC-W) plots (SI Figure S10c,d). Median fluorescence values were determined from 10 000 single-cell events.

To process fluorescence data, the background fluorescence from cells lacking GFP (YEZ140; yMAL248) were subtracted from the fluorescence values of each sample to account for cell autofluorescence and potential light bleaching. All fluorescence measurements were performed once per sample, such that potential activation of VP16-EL222 by the light used to excite GFP or emitted by BFP did not affect our experiments or results.

https://doi.org/10.1021/acssynbio.1c00229
ACS Synth. Biol. XXXX, XXX, XXX−XXX

Construction of Q System Strains. Gene circuits were assembled using restriction enzyme digests and ligations of pJLA vectors as previously described.[43] Strains were constructed by assembling promoter-gene-terminator sequences into single integration vectors targeting the *HIS3* or *LEU2* loci. For acetoin production, the biosynthetic pathway was assembled into multicopy integration vectors targeting δ-sites (YARCdelta5). For geraniol and linalool production, the biosynthetic pathway was assembled into plasmids containing the 2μ origin of replication and *URA3* marker; plasmid selection was maintained using SC−Ura dropout media.

Q System strains and circuits were all characterized in the yeast strain CENPK.2-1C. For crosstalk tests between QF2/QS/$P_{5xQUASf}$ and Gal4p/Gal80p/P_{GAL1}, we used strains derived from YEZ44 (CENPK.2-1C, *gal80*-Δ, *gal4*-Δ) to avoid potential interference from the native copies of *GAL4* and *GAL80*. For crosstalk tests and chemical production using OptoINVRT7, which requires retention of the native copy of *GAL4*, we used strains derived from YEZ25 (CENPK.2-1C, *gal80*-Δ). For chemical production involving optogenetic control of *PDC1*, we used strains derived from YEZ207 (S288C, *pdc1*Δ, *pdc5*Δ, *pdc6*Δ, *gal80*Δ, *gpd1*Δ, *his3::HIS3*$_{cg}$_OptoINVRT7 containing pJLA121PDC1^{0202}).

Characterization of the Q System in *S. cerevisiae*. To characterize P_{5xQUAS}, $P_{5xQUASf}$, and QF2 in *S. cerevisiae*, we integrated linearized pMAL217, pMAL217f, pMAL221, and pMAL221f into the *HIS3* locus of CEN.PK2-1C, creating yMAL49, yMAL49f, yMAL53, and yMAL53f, respectively. We grew 1 mL overnight cultures of YEZ140, YEZ186, yMAL49, yMAL49f, yMAL53, and yMAL53f in SC − His + 2% glucose media in triplicate. We then back-diluted the cultures to OD_{600} = 0.1 in 150 μL triplicates into a 96-well plate and grew the cultures for 6 h. Then, 25 μL from each well was diluted into 175 μL of ice-cold phosphate buffered saline (Corning Life Sciences), kept on ice, and taken for flow cytometry analysis.

To determine the extent of repression of QF2 by QS, we integrated linearized pMAL381, pMAL382, and pMAL570 into the *HIS3* locus of CEN.PK2-1C, creating yMAL110, yMAL111, and yMAL112, respectively. We grew 1 mL overnight cultures of YEZ140, yMAL53f, yMAL110, yMAL111, and yMAL112 in SC − His + 2% glucose media. We then back-diluted the cultures to OD_{600} = 0.1 in 150 μL triplicates into a 96-well plate and grew the cultures for 6 h. Samples were then taken for flow cytometry analysis (as above).

To test inhibition of QS by quinic acid, we grew 1 mL overnight cultures of YEZ140, yMAL110, yMAL111, and yMAL112 in SC − His + 2% glucose media. We then back-diluted the cultures to OD_{600} = 0.1 in 150 μL triplicates into a 96-well plate in SC − His + 2% glucose + 0 mg/L, 50 mg/L, 100 mg/L, 500 mg/L, 1 g/L, 5 g/L, or 10 g/L quinic acid. Acidification of the media from the addition of quinic acid was neutralized to pH = 5 using 5 M KOH. We grew the cultures for 6 h. Samples were then taken for flow cytometry analysis (as above).

To test functionality of qa-y, we integrated linearized pMAL745 into the *HIS3* locus of CEN.PK2-1C, creating yMAL321. We grew overnight 1 mL of cultures of YEZ140, yMAL53f, yMAL112, and yMAL321 in SC − His + 2% glucose media. We then back-diluted the cultures to OD_{600} = 0.1 in 150 μL triplicates into a 96-well plate in SC − His + 2% glucose +0, 1, 5, 10, 50, or 100 mg/L quinic acid. Acidification of the media from addition of quinic acid was neutralized to pH = 5 using 5 M KOH. We grew the cultures for 6 h. Samples were then taken for flow cytometry analysis (as above).

Characterization of OptoQ-INVRT Circuits. To construct OptoQ-INVRT1 and 4, we integrated linearized pMAL513 and pMAL498 into the *HIS3* locus of CEN.PK2-1C, creating yMAL227 and yMAL239, respectively. We grew 1 mL overnight cultures of YEZ140, YEZ186, yMAL227, and yMAL239 in SC − His + 2% glucose media under blue light. We then back-diluted the cultures to OD_{600} = 0.1 in 150 μL triplicates into 96-well plates and grew the cultures for 6 h under continuous (100%) blue light, 10% (10 s ON/90 s OFF) blue light, 1% (1 s ON/99 s OFF) blue light, or darkness (wrapped in aluminum foil). Samples were then taken for flow cytometry analysis (as above).

To compare the kinetics of OptoQ-INVRT circuits, we grew 1 mL overnight cultures of YEZ140, yMAL227, yMAL239, and YEZ230 (OptoINVRT7 with $P_{GAL1\text{-}M}$-GFP) in SC − His + 2% glucose media under blue light. We back-diluted the cultures to OD_{600} = 0.1 in 1 mL triplicates in eight separate 24-well plates and grew the cultures for 3 h under blue light, at which point the cultures reached OD_{600} = 0.8. We then switched six plates to the dark (by wrapping in aluminum foil); one plate was left in blue light for 8 h as a control and another was processed immediately (0 h time point). After 0, 1, 2, 3, 4, 6, and 8 h in the dark, 25 μL from each well was diluted into 175 μL of ice-cold phosphate buffered saline, kept on ice, and taken for flow cytometry analysis (as above).

To calculate the half-activation time of each circuit, we constructed a trendline using the linear portion of each activation curve and used it to calculate the time at which half of the GFP maximum was reached (i.e., calculated the time (x) value at which GFP (y) = $GFP_{max}/2$). To calculate the time delay, we found the x-intercept of the trendline (i.e., calculated the time (x) value at which GFP (y) = 0).

Characterization of OptoQ-AMP circuits. To construct OptoQ-AMP1-6, we integrated linearized pMAL358, pMAL669, pMAL722, pMAL716, pMAL724, and pMAL728 into the *HIS3* locus of CEN.PK2-1C, creating yMAL176, yMAL273, yMAL299, yMAL298, yMAL301, and yMAL305, respectively. We grew 1 mL overnight cultures of YEZ140, YEZ186, yMAL176, yMAL273, yMAL299, yMAL298, yMAL301, and yMAL305 in SC − His + 2% glucose media in the dark. We then back-diluted the cultures to OD_{600} = 0.1 in 150 μL triplicates into 96-well plates and grew the cultures for 6 h under continuous (100%) blue light, 10% (10 s ON/90 s OFF) blue light, 1% (1 s ON/99 s OFF) blue light, or darkness (wrapped in aluminum foil). Samples were then taken for flow cytometry analysis (as above).

To investigate how the strength of the promoter driving QS_PSD expression impacts circuit performance, we integrated linearized pMAL609 and pMAL723 into the *HIS3* locus of CEN.PK2-1C, creating yMAL243 and yMAL300, respectively. We grew 1 mL overnight cultures of YEZ140, YEZ186, yMAL299, yMAL243, yMAL300, and yMAL305 in SC − His + 2% glucose media in the dark. We then back-diluted the cultures to OD_{600} = 0.1 in 150 μL triplicates into 96-well plates in SC − His + 2% glucose and grew the cultures for 6 h under continuous (100%) blue light, 10% (10 s ON/90 s OFF) blue light, 1% (1 s ON/99 s OFF) blue light, or darkness (wrapped in aluminum foil). Samples were then taken for flow cytometry analysis (as above).

To compare the kinetics of OptoQ-AMP1, OptoQ-AMP3, and OptoAMP1, we grew 1 mL overnight cultures of YEZ140,

https://doi.org/10.1021/acssynbio.1c00229
ACS Synth. Biol. XXXX, XXX, XXX−XXX

yMAL176, yMAL299, and YEZ72 (OptoAMP1 with P_{GAL1}_GFP) in SC − His + 2% glucose in the dark. We then back-diluted the cultures to OD_{600} = 0.1 in 1 mL triplicates in four separate 24-well plates and grew the cultures for 3 h in darkness (covered with aluminum foil), at which point the cultures reached OD_{600} = 1. We then exposed the plates to blue light. After 0, 1, 2, and 3 h of illumination, 25 μL from each well was diluted into 175 μL of ice-cold phosphate buffered saline, kept on ice, and taken for flow cytometry analysis (as above).

To compare the kinetics of OptoQ-AMP1, OptoQ-AMP2, OptoQ-AMP4, OptoQ-AMP5, and OptoQ-AMP6, we grew in the dark 1 mL overnight cultures of YEZ140, yMAL176, yMAL273, yMAL298, yMAL301, and yMAL305 in SC − His + 2% glucose. We then back-diluted the cultures to OD_{600} = 0.1 in 1 mL triplicates in eight separate 24-well plates and grew the cultures for 3 h in darkness, at which point the cultures reached OD_{600} = 1. We then exposed 7 of the plates to blue light; one plate was left in darkness for 12 h as a control. After 0, 2, 4, 6, 8, 10, and 12 h of illumination, 25 μL from each well was diluted into 175 μL of ice-cold phosphate buffered saline, kept on ice, and taken for flow cytometry analysis (as above).

Characterization of Potential Cross-Talk between GAL and qa Regulons. To test for cross-talk between QF2, Gal4p, and Gal80p, we integrated linearized pMAL217f, pMAL221f, pMAL398, and pMAL380 into the *HIS3* locus of YEZ44, creating yMAL207, yMAL268, yMAL195, and yMAL198, respectively. We grew 1 mL overnight cultures of YEZ140, yMAL207, yMAL268, yMAL195, and yMAL198 in SC − His + 2% glucose media. We then back-diluted the cultures to OD_{600} = 0.1 in 150 μL triplicates into a 96-well plate and grew the cultures for 6 h. Samples were then taken for flow cytometry analysis (as above).

To test for cross-talk between Gal4p, QF2, and QS, we integrated linearized EZ-L164, pMAL397, pMAL374, and pMAL379 into the *HIS3* locus of YEZ44, creating YEZ82, yMAL194, yMAL251, and yMAL197, respectively. We grew 1 mL overnight cultures of YEZ140, YEZ82, yMAL194, yMAL251, and yMAL197 in SC − His + 2% glucose media. We then back-diluted the cultures to OD_{600} = 0.1 in 150 μL triplicates into a 96-well plate and grew the cultures for 6 h. Samples were then taken for flow cytometry analysis (as above).

To confirm that OptoINVRT and OptoQ-AMP could be used in the same strain without cross-talk, we integrated linearized pMAL592 (OptoQ-AMP1 driving $P_{5xQUASf}$_BFP) into the *LEU2* locus of YEZ230 (OptoINVRT7 driving $P_{GAL1\text{-}M}$_GFP in the *HIS3* locus), creating yMAL246. This strain should only show GFP expression in darkness, and TagBFP expression in blue light. To make a control strain to subtract autofluorescence in which neither GFP nor BFP are expressed, we integrated linearized EZ-L439 (OptoINVRT7) into the *HIS3* locus of YEZ25, creating yMAL155. We then integrated linearized pMAL743 (OptoQ-AMP1) into the *LEU2* locus of yMAL155, creating yMAL248. To make a strain that controls only GFP expression, we integrated linearized pMAL743 into the *LEU2* locus of YEZ230, creating yMAL245. To make a strain that controls only BFP expression, we integrated linearized pMAL592 into the *LEU2* locus of yMAL155, creating yMAL249. To make a positive control that expresses both GFP and TBFP constitutively as a test for potential fluorophore photobleaching, we integrated linearized pMAL653 (P_{TEF1}_BFP) into the *LEU2* locus of YEZ186 (which already contains P_{TEF1}_GFP), creating yMAL270. Overnight cultures of yMAL270, yMAL245, yMAL246, yMAL248, and yMAL249 were grown in darkness in SC − His − Leu + 2% glucose. Cultures were then back-diluted to OD_{600} = 0.1 in 150 μL triplicates into 96-well plates and grown for 6 h under blue light or darkness (plates wrapped in aluminum foil). Samples were then taken for flow cytometry analysis (as above).

Construction and Screening of Acetoin Producing Strains. To construct a strain that allows for optogenetic control over cellular growth, we integrated linearized pMAL566 (OptoQ-AMP1 driving *PDC1*) into YEZ207, then counter-selected against plasmid *pJLA121-PDC1*^{0202} using 5-FOA, creating yMAL241. To verify that this strain could only grow under blue light, we inoculated overnight cultures of CEN.PK2-1C and yMAL241 in SC + 2% glucose media under blue light. Each culture was then diluted to 0.01 OD_{600} and grown at 30 °C, 200 rpm, either under continuous (100%) blue light or in darkness (wrapped in aluminum foil), taking OD_{600} measurements until reaching steady state. We then deleted the *BDH1* gene (which converts acetoin into 2,3-butanediol) from yMAL241, creating strain yMAL311.

Plasmids pMAL557 and pMAL558 contain the acetoin biosynthetic pathway,[27] α-acetolactate synthase (AlsS) and α-acetolactate decarboxylase (AlsD) from *Bacillus subtilis*, for multicopy integration into δ-sites (YARCdelta5) within the yeast genome. The first gene in the pathway, *alsS*, is expressed constitutively using P_{TDH3} (pMAL557) or in darkness using $P_{GAL1\text{-}S}$ (pMAL558). We integrated linearized pMAL558 into yMAL311, creating yMAL322. To make a control strain that lacks optogenetic regulation of acetoin production, we integrated linearized pMAL557 into yMAL311, creating yMAL323. Transformants were plated on YPD agar overnight and grown under full blue light. The next day, colonies were replica plated onto YPD agar supplemented with 1200 μg/mL Zeocin.

To make a control strain that lacks optogenetic control of growth, we removed *pJLA121-PDC1*^{0202} from YEZ207 using 5-FOA and then restored the endogenous copy of *PDC1* (in its original locus), creating yMAL327. We integrated linearized OptoQ-AMP1 (pMAL743) into the *LEU2* locus, creating yMAL328. We then deleted *BDH1* from yMAL328, creating yMAL331. Finally, we integrated linearized pMAL558 into the δ-sites of yMAL331, creating yMAL332. To make a control strain that lacks optogenetic control of both growth and production, we integrated linearized pMAL557 into the δ-sites of yMAL331, creating yMAL364. Transformants were plated on YPD agar overnight; transformants for yMAL332 were grown under full blue light to avoid potential negative selection due to pathway expression. The next day, colonies were replica plated onto YPD agar supplemented with 1200 μg/mL Zeocin.

Eight colonies from each transformation plate were screened for acetoin production. Each colony was used to inoculate 1 mL of SC + 2% glucose media in 24-well plates and grown overnight under blue light. We then back-diluted the cultures to OD_{600} = 0.1 and grew them under blue light for approximately 6 h, at which point OD_{600} = 1.5. At this point, the plates were wrapped in aluminum foil and the cultures were incubated in the dark for 2 h as previously described.[4] The cultures were then centrifuged in a Sorvall Legend XTR at 2000 rpm for 10 min and resuspended in fresh SC + 2% glucose media. Plates were then sealed with Sealing Tape (Excel Scientific, Victorville, CA, U.S.A.; Catalog No.

https://doi.org/10.1021/acssynbio.1c00229
ACS Synth. Biol. XXXX, XXX, XXX−XXX

STR-SEAL-PLT) and incubated in the dark for 48 h. Cultures were harvested and centrifuged at 2000 rpm for 10 min. Supernatants were analyzed with GC-FID as described below. The highest producing colonies of yMAL322, yMAL323, and yMAL332 were selected for subsequent optimization.

To find the optimal cell density at which to switch cultures from light to dark, ρ_s, we grew overnight cultures of yMAL322, yMAL323, and yMAL332 under blue light in SC + 2% glucose. We then back-diluted the cultures to different initial OD_{600} values, ranging from 0.01 to 0.2, in 1 mL quadruplicates. The strains were then grown for approximately 12 h under continuous blue light, at which point OD_{600} = 0.2−3.9. We then incubated the cultures in the dark for 2 h. The cultures were then centrifuged in a Sorvall Legend XTR at 2000 rpm for 10 min and resuspended in fresh SC + 2% glucose media. Plates were then sealed with sealing tape and incubated in the dark for 48 h. Control cultures were grown under constant blue light throughout the fermentation. Cultures were harvested and centrifuged at 2000 rpm for 10 min. Supernatants were analyzed with GC-FID as described below.

To investigate the benefit of pulsing light during the production phase of high glucose fermentations, we grew overnight cultures of yMAL322, yMAL323, and yMAL332 under blue light in SC + 2% glucose. We then back-diluted the cultures to OD_{600} = 0.1 in 1 mL triplicates and grew them under blue light for approximately 4 h at which point OD_{600} = 0.2−0.5. We then incubated the cultures in the dark for 2 h. The cultures were then centrifuged in a Sorvall Legend XTR at 2000 rpm for 10 min and resuspended in fresh SC + 15% glucose media. Plates were then sealed with sealing tape and incubated for 96 h under the light schedule: 4 h of constant blue light, followed by blue light pulses of 10 s ON/90 s OFF for 30 min every 2, 6, or 10 h. Control cultures were grown under constant blue light or darkness following resuspension in fresh media. Cultures were harvested and centrifuged at 2000 rpm for 10 min. Supernatants were analyzed with GC-FID as described below.

Construction and Screening of Geraniol and Linalool Producing Strains. To investigate tunability of different proteins (GFP and BFP) in a single strain using light duty cycle, we grew 1 mL overnight cultures of yMAL248 and yMAL246 in SC − His − Leu + 2% glucose media in the dark. We then back-diluted the cultures to OD_{600} = 0.1 in 150 μL triplicates into 96-well plates and grew the cultures for 6 h under continuous (100%) blue light, 10% (10 s ON/90 s OFF) blue light, 1% (1 s ON/99 s OFF) blue light, or darkness (wrapped in aluminum foil). Samples were then taken for flow cytometry analysis (as above).

To construct a strain that allows for optogenetic control over geraniol and linalool production, we integrated OptoQ-AMP4 (pMAL741) into the *LEU2* locus of yMAL155, creating yMAL310. We then transformed yMAL310 with pMAL778, containing P_{TDH3} driving constitutive expression of a mutant farnesyl diphosphate synthase (*ERG20*^{F96C}),[46] $P_{5xQUASf}$ controlling expression of geraniol synthase from *Ocimum basilicum* (ObGES),[28] and $P_{GAL1\text{-}S}$ controlling expression of linalool synthase from *Mentha citrata* (McLIS),[28] to create yMAL360.

Eight colonies of yMAL360 were screened for geraniol and linalool production. Each colony was used to inoculate 1 mL of SC − Ura + 2% glucose media in a 24-well plate and grown overnight under 10% (10 s ON/90 s OFF) blue light. We then back-diluted the cultures to OD_{600} = 0.2 into 1 mL of fresh SC − Ura + 2% glucose. An overlay of 100 μL of dodecane was added to each well, and the plates were sealed with sealing tape and incubated under blue light (to measure production of geraniol) or in the dark (to measure production of linalool) for 48 h. Cultures were then harvested and supernatants were analyzed with GC-MS as described below. The highest producing colony of yMAL360 (in terms of total geraniol + linalool titer) was selected for subsequent optimization.

We then analyzed changes in geraniol and linalool production under different light pulses. We grew overnight cultures of yMAL360 under 10% (10 s ON/90 s OFF) blue light in SC − Ura + 2% glucose. We then back-diluted the cultures to OD_{600} = 0.2 in 1 mL quadruplicates into fresh SC − Ura + 2% glucose. An overlay of 100 μL of dodecane was added to each well, and the plates were sealed with sealing tape and incubated under continuous blue light, 10% (10 s ON/90 s OFF) blue light, 1% (1s ON/99 s OFF) blue light, or darkness (wrapped in aluminum foil) for 48 h. Cultures were then harvested and supernatants were analyzed with GC-MS as described below.

Fermentations and Analytical Methods. For acetoin production, cultures were centrifuged in a Sorvall Legend XTR at 2000 rpm for 10 min at 4 °C. 500 μL of cell-free supernatant was mixed with 1 mL of ethyl acetate in a 2 mL microcentrifuge tube and vortexed for 20 min, then spun down at 17 000 RCF in an Eppendorf 5424 microcentrifuge for 15 min at 4 °C. Then, 500 μL of the organic phase was transferred to an autosampler vial for analysis. For linalool and geraniol, the entire sample (culture + overlay) was mixed with 1 mL of ethyl acetate for extraction; subsequent steps are the same as above.

Concentrations of acetoin, geraniol, and linalool were quantified using an Agilent 7890B GC System equipped with a flame ionization detector and an Agilent 5977A MSD. To determine analyte concentrations, the peak areas were measured and compared to those of standard solutions for quantification. For acetoin, samples were injected and subjected to a split (0.5 μL injection volume; 1:20 split), using a constant helium flow of 1.5 mL/min. Samples were separated using a DB-Wax column (30 m length, 0.25 mm diameter, 0.5 μm film) and a gradient as follows: Initial oven temperature was set to 70 °C and held for 3 min, and temperature was then ramped at a rate of 20 °C/min to 230 °C and held for 5 min. Samples were quantified using flame-ionization detection (300 °C, H_2 flow 30 mL/min, air flow 400 mL/min, makeup flow 25 mL/min) and compared to a commercial standard. For geraniol and linalool, samples were injected (1 μL) in splitless mode with a constant helium flow of 1.5 mL/min. Samples were separated using a DB-Wax column and a gradient as follows: Initial oven temperature was set to 70 °C and held for 3 min, temperature was then ramped at a rate of 20 °C/min to 230 °C and held for 5 min. Samples were analyzed using selected ion monitoring for the following ions based on available spectra: linalool (71, 93, 121 *m*/*z*, 100 ms dwell time) and geraniol (41, 69, 123 *m*/*z*, 100 ms dwell time) with monitoring windows based on retention times of commercially available standards.

■ ASSOCIATED CONTENT

Supporting Information

The Supporting Information is available free of charge at https://pubs.acs.org/doi/10.1021/acssynbio.1c00229.

https://doi.org/10.1021/acssynbio.1c00229
ACS Synth. Biol. XXXX, XXX, XXX−XXX

Sequences of engineered promoters; characterization of Q System promoter variants and quinic acid response; tuning and characterization of optogenetic circuits; growth curve of a light-dependent strain; optimization of light-controlled fermentations; plasmid assembly diagram; flow cytometry gating; tables of plasmids and strains (PDF)

AUTHOR INFORMATION

Corresponding Author

José L. Avalos − *Department of Chemical and Biological Engineering, Department of Molecular Biology, and The Andlinger Center for Energy and the Environment, Princeton University, Princeton, New Jersey 08544, United States;* orcid.org/0000-0002-7209-4208; Email: javalos@princeton.edu

Authors

Makoto A. Lalwani − *Department of Chemical and Biological Engineering, Princeton University, Princeton, New Jersey 08544, United States;* orcid.org/0000-0003-4629-4131

Evan M. Zhao − *Department of Chemical and Biological Engineering, Princeton University, Princeton, New Jersey 08544, United States*

Scott A. Wegner − *Department of Molecular Biology, Princeton University, Princeton, New Jersey 08544, United States*

Complete contact information is available at: https://pubs.acs.org/10.1021/acssynbio.1c00229

Author Contributions

M.A.L. and J.L.A. conceived this project and designed the experiments. M.A.L. and E.M.Z. constructed the strains and plasmids. M.A.L. and S.A.W. executed the experiments. M.A.L. and J.L.A. analyzed the data and wrote the paper.

Funding

J.L.A is supported by the U.S. Department of Energy, Office of Science, Office of Biological and Environmental Research Award Number DE-SC0019363, the NSF CAREER Award CBET-1751840, The Pew Charitable Trusts, the Camille Dreyfus Teacher-Scholar Award and Princeton SEAS Project-X.

Notes

The authors declare no competing financial interest.

ACKNOWLEDGMENTS

We are grateful to Dr. Christopher Potter for answering our inquiries regarding the Q System. We thank Dr. Christina DeCoste, Dr. Katherine Rittenbach, and the Princeton Molecular Biology Flow Cytometry Resource Center for assistance with flow cytometry experiments. The shapes for QS, QF2, the 96-well plate, and beer mug in the TOC figure were made with BioRender.

REFERENCES

(1) Toettcher, J. E., Voigt, C. A., Weiner, O. D., and Lim, W. A. (2011) The promise of optogenetics in cell biology: interrogating molecular circuits in space and time. *Nat. Methods 8*, 35−38.

(2) Figueroa, D., Rojas, V., Romero, A., Larrondo, L. F., and Salinas, F. (2021) The rise and shine of yeast optogenetics. *Yeast 38*, 131−146.

(3) Motta-Mena, L. B., Reade, A., Mallory, M. J., Glantz, S., Weiner, O. D., Lynch, K. W., and Gardner, K. H. (2014) An optogenetic gene expression system with rapid activation and deactivation kinetics. *Nat. Chem. Biol. 10*, 196−202.

(4) Zhao, E. M., Zhang, Y., Mehl, J., Park, H., Lalwani, M. A., Toettcher, J. E., and Avalos, J. L. (2018) Optogenetic regulation of engineered cellular metabolism for microbial chemical production. *Nature 555*, 683−687.

(5) Zhao, E. M., Lalwani, M. A., Chen, J., Orillac, P., Toettcher, J. E., and Avalos, J. L. (2021) Optogenetic Amplification Circuits for Light-Induced Metabolic Control. *ACS Synth. Biol. 10*, 1143.

(6) Giles, N. H., Case, M. E., Baum, J., Geever, R., Huiet, L., Patel, V., and Tyler, B. (1985) Gene organization and regulation in the qa (quinic acid) gene cluster of Neurospora crassa. *Microbiol. Rev. 49*, 338−58.

(7) Baum, J. A., Geever, R., and Giles, N. H. (1987) Expression of qa-1F activator protein: identification of upstream binding sites in the qa gene cluster and localization of the DNA-binding domain. *Mol. Cell. Biol. 7*, 1256−1266.

(8) Geever, R. F., Huiet, L., Baum, J. A., Tyler, B. M., Patel, V. B., Rutledge, B. J., Case, M. E., and Giles, N. H. (1989) DNA sequence, organization and regulation of the qa gene cluster of Neurospora crassa. *J. Mol. Biol. 207*, 15−34.

(9) Arnett, D. R., Lorimer, H. E., and Asch, D. K. (2009) Catabolite repression directly affects transcription of the qa-y gene of Neurospora crassa. *Fungal Genet. Biol. 46*, 377−380.

(10) Mozsik, L., Buttel, Z., Bovenberg, R. A. L., Driessen, A. J. M., and Nygard, Y. (2019) Synthetic control devices for gene regulation in Penicillium chrysogenum. *Microb. Cell Fact. 18*, 1−13.

(11) Potter, C. J., Tasic, B., Russler, E. V., Liang, L., and Luo, L. (2010) The Q system: A repressible binary system for transgene expression, lineage tracing, and mosaic analysis. *Cell 141*, 536−548.

(12) Wei, X., Potter, C. J., Luo, L., and Shen, K. (2012) Controlling gene expression with the Q repressible binary expression system in Caenorhabditis elegans. *Nat. Methods 9*, 391−395.

(13) Subedi, A., Macurak, M., Gee, S. T., Monge, E., Goll, M. G., Potter, C. J., Parsons, M. J., and Halpern, M. E. (2014) Adoption of the Q transcriptional regulatory system for zebrafish transgenesis. *Methods 66*, 433−440.

(14) Riabinina, O., Task, D., Marr, E., Lin, C. C., Alford, R., O'Brochta, D. A., and Potter, C. J. (2016) Organization of olfactory centres in the malaria mosquito Anopheles gambiae. *Nat. Commun. 7*, 13010 DOI: 10.1038/ncomms13010.

(15) Fitzgerald, M., Gibbs, C., Shimpi, A. A., and Deans, T. L. (2017) Adoption of the Q Transcriptional System for Regulating Gene Expression in Stem Cells. *ACS Synth. Biol. 6*, 2014−2020.

(16) Persad, R., Reuter, D. N., Dice, L. T., Nguyen, M. A., Rigoulot, S. B., Layton, J. S., Schmid, M. J., Poindexter, M. R., Occhialini, A., Stewart, C. N., and Lenaghan, S. C. (2020) The Q-System as a Synthetic Transcriptional Regulator in Plants. *Front. Plant Sci. 11*, 1−12.

(17) Riabinina, O., Luginbuhl, D., Marr, E., Liu, S., Wu, M. N., Luo, L., and Potter, C. J. (2015) Improved and expanded Q-system reagents for genetic manipulations. *Nat. Methods 12*, 219−222.

(18) Skjoedt, M. L., Snoek, T., Kildegaard, K. R., Arsovska, D., Eichenberger, M., Goedecke, T. J., Rajkumar, A. S., Zhang, J., Kristensen, M., Lehka, B. J., Siedler, S., Borodina, I., Jensen, M. K., and Keasling, J. D. (2016) Engineering prokaryotic transcriptional activators as metabolite biosensors in yeast. *Nat. Chem. Biol. 12*, 951−958.

(19) Lee, M. E., DeLoache, W. C., Cervantes, B., and Dueber, J. E. (2015) A Highly Characterized Yeast Toolkit for Modular, Multipart Assembly. *ACS Synth. Biol. 4*, 975−986.

(20) Chaleff, R. S. (2000) The inducible quinate-shikimate catabolic pathway in Neurospora crassa: induction and regulation of enzyme synthesis. *Microbiology 81*, 357−372.

(21) Zhao, E. M., Lalwani, M. A., Lovelett, R. J., García-Echaurí, S. A., Hoffman, S. M., Gonzalez, C. G., Toettcher, J. E., Kevrekidis, I. G., and Avalos, J. L. (2020) Design and characterization of rapid optogenetic circuits for dynamic control in yeast metabolic engineering. *ACS Synth. Biol. 9*, 3254−3266.

(22) Jungbluth, M., Renicke, C., and Taxis, C. (2010) Targeted protein depletion in Saccharomyces cerevisiae by activation of a bidirectional degron. *BMC Syst. Biol. 4*, 176.
(23) Rivera-Cancel, G., Motta-Mena, L. B., and Gardner, K. H. (2012) Identification of natural and artificial DNA substrates for light-activated LOV-HTH transcription factor EL222. *Biochemistry 51*, 10024−10034.
(24) Usherenko, S., Stibbe, H., Muscò, M., Essen, L.-O. O., Kostina, E. A., and Taxis, C. (2014) Photo-sensitive degron variants for tuning protein stability by light. *BMC Syst. Biol. 8*, 128.
(25) Flikweert, M. T., van der Zanden, L., Janssen, W. M. T. M., Yde Steensma, H., van Dijken, J. P., and Pronk, J. T. (1996) Pyruvate Decarboxylase: An Indispensable Enzyme for Growth of Saccharomyces cerevisiae on Glucose. *Yeast 12*, 247−257.
(26) Sakai, A., Shimizu, Y., and Hishinuma, F. (1990) Integration of heterologous genes into the chromosome of Saccharomyces cerevisiae using a delta sequence of yeast retrotransposon Ty. *Appl. Microbiol. Biotechnol. 33*, 302−306.
(27) Bae, S.-J., Kim, S., and Hahn, J.-S. (2016) Efficient production of acetoin in Saccharomyces cerevisiae by disruption of 2,3-butanediol dehydrogenase and expression of NADH oxidase. *Sci. Rep. 6*, 27667.
(28) Denby, C. M., Li, R. A., Vu, V. T., Costello, Z., Lin, W., Chan, L. J. G., Williams, J., Donaldson, B., Bamforth, C. W., Petzold, C. J., Scheller, H. V., Martin, H. G., and Keasling, J. D. (2018) Industrial brewing yeast engineered for the production of primary flavor determinants in hopped beer. *Nat. Commun. 9*, 1−10.
(29) Zhou, P., Du, Y., Xu, N., Yue, C., and Ye, L. (2020) Improved linalool production in Saccharomyces cerevisiae by combining directed evolution of linalool synthase and overexpression of the complete mevalonate pathway. *Biochem. Eng. J. 161*, 107655.
(30) Zhou, P., Du, Y., Fang, X., Xu, N., Yue, C., and Ye, L. (2021) Combinatorial Modulation of Linalool Synthase and Farnesyl Diphosphate Synthase for Linalool Overproduction in Saccharomyces cerevisiae. *J. Agric. Food Chem. 69*, 1003−1010.
(31) Cann, A. F., and Liao, J. C. (2008) Production of 2-methyl-1-butanol in engineered Escherichia coli. *Appl. Microbiol. Biotechnol. 81*, 89−98.
(32) Hammer, S. K., Zhang, Y., and Avalos, J. L. (2020) Mitochondrial Compartmentalization Confers Specificity to the 2-Ketoacid Recursive Pathway: Increasing Isopentanol Production in Saccharomyces cerevisiae. *ACS Synth. Biol. 9*, 546−555.
(33) Gold, N. D., Gowen, C. M., Lussier, F.-X., Cautha, S. C., Mahadevan, R., and Martin, V. J. J. (2015) Metabolic engineering of a tyrosine-overproducing yeast platform using targeted metabolomics. *Microb. Cell Fact. 14*, 73.
(34) Kunjapur, A. M., and Eldridge, R. B. (2010) Photobioreactor design for commercial biofuel production from microalgae. *Ind. Eng. Chem. Res. 49*, 3516−3526.
(35) Chen, C. Y., Yeh, K. L., Aisyah, R., Lee, D. J., and Chang, J. S. (2011) Cultivation, photobioreactor design and harvesting of microalgae for biodiesel production: A critical review. *Bioresour. Technol. 102*, 71−81.
(36) Delgado, J., and Liao, J. C. (1995) Control of metabolic pathways by time-scale separation. *BioSystems 36*, 55−70.
(37) Carrasco-López, C., García-Echauri, S. A., Kichuk, T., and Avalos, J. L. (2020) Optogenetics and biosensors set the stage for metabolic cybergenetics. *Curr. Opin. Biotechnol. 65*, 296−309.
(38) Shimizu-Sato, S., Huq, E., Tepperman, J. M., and Quail, P. H. (2002) A light-switchable gene promoter system. *Nat. Biotechnol. 20*, 1041−1044.
(39) Pathak, G. P., Strickland, D., Vrana, J. D., and Tucker, C. L. (2014) Benchmarking of optical dimerizer systems. *ACS Synth. Biol. 3*, 832−838.
(40) Kaberniuk, A., Shemetov, A. A., and Verkhusha, V. V. (2016) A bacterial phytochrome-based optogenetic system controllable with near-infrared light. *Nat. Methods 13*, 591−597.
(41) Redchuk, T. A., Omelina, E. S., Chernov, K. G., and Verkhusha, V. V. (2017) Near-infrared optogenetic pair for protein regulation and spectral multiplexing. *Nat. Chem. Biol. 13*, 633−639.
(42) Lovelett, R. J., Zhao, E. M., Lalwani, M. A., Toettcher, J. E., Kevrekidis, I. G., and Avalos, J. L. (2021) Dynamical Modeling of Optogenetic Circuits in Yeast for Metabolic Engineering Applications. *ACS Synth. Biol. 10*, 219−227.
(43) Avalos, J. L., Fink, G. R., and Stephanopoulos, G. (2013) Compartmentalization of metabolic pathways in yeast mitochondria improves the production of branched-chain alcohols. *Nat. Biotechnol. 31*, 335−341.
(44) Gibson, D. G, Young, L., Chuang, R.-Y., Venter, J C., Hutchison, C. A, and Smith, H. O (2009) Enzymatic assembly of DNA molecules up to several hundred kilobases. *Nat. Methods 6*, 343−345.
(45) Gietz, R. D., and Woods, R. A. (2002) Transformation of yeast by lithium acetate/single-stranded carrier DNA/polyethylene glycol method. *Methods Enzymol. 350*, 87−96.
(46) Dong, H., Chen, S., Zhu, J., Gao, K., Zha, W., Lin, P., and Zi, J. (2020) Enhance production of diterpenoids in yeast by over-expression of the fused enzyme of ERG20 and its mutant mERG20. *J. Biotechnol. 307*, 29−34.

https://doi.org/10.1021/acssynbio.1c00229
ACS Synth. Biol. XXXX, XXX, XXX−XXX